[redacted]

TRW

# TAPCO GROUP

## *Thompson Ramo Wooldridge Inc.*

Cleveland 17, Ohio

Special Distribution

TAPCO GROUP Thompson Ramo Wooldridge Inc.

MND-P-2378
ENGINEERING REPORT 4053

# SNAP I POWER CONVERSION SYSTEM

# PUMP DEVELOPMENT

PREPARED BY

NEW DEVICES LABORATORIES, TAPCO GROUP

THOMPSON RAMO WOOLDRIDGE INC.

AS AUTHORIZED BY

THE MARTIN CO. PURCHASE ORDER 0E 0101

FOR

THE UNITED STATES ATOMIC ENERGY COMMISSION

PRIME CONTRACT AT(30-3)-217

1 FEBRUARY 1957 TO 30 JUNE 1959

PUBLISHED

JUNE 20, 1960

PREPARED BY: E. S. KOVALCIK
D. C. REEMSNYDER

## LEGAL NOTICE

## DISTRIBUTION LIST

| | | Copy No. |
|---|---|---|
| 1. | Commander, AFBMD<br>Hq., USAF ARDL<br>P.O. Box 262<br>Inglewood, California<br>For: Maj. G. Austin | 1 |
| 2. | Commander, ARDC<br>Andrews Air Force Base<br>Washington 25, D. C.<br>Attn: RDTAPS, Capt. W. G. Alexander | 2 |
| 3. | Army Ballistic Missile Agency<br>Commanding General<br>Army Ballistic Missile Agency<br>Redstone Arsenal, Alabama<br>Attn: ORDAB-c | 3, 4 |
| 4. | U. S. Atomic Energy Commission<br>Technical Reports Library<br>Washington 25, D. C.<br>Attn: Mr. J. M. O'Leary<br>For: Lt. Col. G. M. Anderson, DRD<br><br>Capt. John P. Wittry, DRD<br>Lt. Col. Robert D. Cross, DRD<br>R. G. Oehl, DRD<br>Edward F. Miller, PROD<br>Technical Reports Library | 5 through 10 |
| 5. | Atomics International<br>Division of North American Aviation, Inc.<br>P. O. Box 309, Canoga Park, California<br>Attn: Dr. Chauncey Starr<br>For: J. Wetch | 11 |
| 6. | Chief, Bureau of Aeronautics<br>Washington 25, D. C.<br>Attn: C. L. Gerhardt, NP | 12 |

## DISTRIBUTION LIST (Continued)

| | | Copy No. |
|---|---|---|
| 7. | Chief, Bureau of Ordnance<br>Dept. of the Navy, 4110 Main Navy Bldg.<br>Washington 25, D. C.<br>Attn: Mrs. R. Schmidt or G. Myers<br>To be opened by addressee only for: Ren, SP | 13, 14 |
| 8. | Chief, Bureau of Ships<br>Department of the Navy, Code 1500<br>Washington 25, D. C.<br>Attn: Melvin L. Ball | 15 |
| 9. | U. S. Atomic Energy Commission<br>Canoga Park Area Office<br>P. O. Box 591<br>Canoga Park, California<br>Attn: A. P. Pollman, Area Manager | 16 |
| 10. | U. S. Atomic Energy Commission<br>Chicago Operations Office<br>P. O. Box 59, Lemont, Ill.<br>Attn: A. I. Mulyck<br>For T. A. Nemzek, Mr. Klein | 17, 18 |
| 11. | Office of the Chief of Naval Operations<br>Department of the Navy<br>Washington 25, D. C. | 19 |
| 12. | Atomic Division<br>Office of Chief of Research & Development<br>Department of the Army<br>Washington 25, D. C. | 20 |
| 13. | Commanding Officer<br>Diamond Ordnance Fuse Laboratories<br>Washington 25, D. C.<br>Attn: ORDTL 06.33, Mrs. M. A. Hawkins | 21 through 23 |

## DISTRIBUTION LIST (Continued)

| | | Copy No. |
|---|---|---|
| 14. | U. S. Atomic Energy Commission<br>Hanford Operations Office<br>P. O. Box 550<br>Richland, Washington<br>Attn: Technical Information Library | 24 |
| 15. | Lockheed Aircraft Corporation<br>Missile Systems Division<br>Palo Alto, California<br>Attn: Mr. Hal H. Greenfield | 25, 26 |
| 16. | Monsanto Chemical Company<br>Mound Laboratory<br>P. O. Box 32, Miamisburg, Ohio<br>Attn: Library and Records Center<br>For: Mr. Roberson | 27 |
| 17. | National Aeronautics & Space Administration<br>Ames Aeronautical Laboratory<br>Moffett Field, California<br>Attn: Smith J. de France, Director | 28 |
| 18. | National Aeronautics & Space Administration<br>Langley Aeronautical Laboratory<br>Langley Field, Virginia<br>Attn: Henry J. E. Reid, Director | 29 |
| 19. | National Aeronautics & Space Administration<br>Lewis Flight Propulsion Laboratory<br>21000 Brookpark Road<br>Cleveland 35, Ohio<br>Attn: George Mandel | 30 |
| 20. | Commander<br>U. S. Naval Ordnance Laboratory<br>White Oak, Silver Spring, Maryland<br>Attn: Eva Lieberman, Librarian | 31 through 33 |

## DISTRIBUTION LIST (Continued)

| | | Copy No. |
|---|---|---|
| 21. | Director<br>Naval Research Laboratory, Code 1572<br>Washington 25, D. C.<br>Attn: Mrs. Katherine H. Cass | 34 |
| 22. | U. S. Atomic Energy Commission<br>New York Operations Office<br>376 Hudson Street<br>New York 14, New York<br>Attn: Reports Librarian | 35, 84 |
| 23. | Union Carbide Nuclear Company<br>X-10, Laboratory Records Department<br>P. O. Box X<br>Oak Ridge, Tennessee<br>Attn: Eugene Lamb | 36 |
| 24. | Office of Naval Research<br>Department of the Navy, Code 735<br>Washington 25, D. C.<br>Attn: E. E. Sullivan<br>For: Code 429 | 37 |
| 25. | Director, USAF Project Rand<br>Via AF Liaison Of., The Rand Corporation<br>1700 Main St., Santa Monica, California<br>Attn: F. R. Collbohm<br>For: Dr. J. Huth | 38 |
| 26. | Commander, Rome Air Development Center<br>Griffiss Air Force Base, New York<br>Attn: RCSG, J. L. Briggs | 39 |
| 27. | U. S. Atomic Energy Commission<br>Reference Branch<br>Technical Information Service Extension<br>Oak Ridge, Tennessee | 40 through 64 |

DISTRIBUTION LIST (Continued)

| | | Copy No. |
|---|---|---|
| 28. | Thompson Ramo Wooldridge<br>Staff Research and Development<br>New Devices Laboratories<br>P. O. Box 1610, Cleveland 4, Ohio | 65, 66, 67 |
| 29. | Univ. of Calif. Radiation Lab<br>Technical Information Division<br>P. O. Box 808, Livermore, Calif.<br>Attn: C. G. Craig<br>For: Dr. H. Gordon | 68 |
| 30. | Commander, Wright Air Dev. Center<br>Wright-Patterson Air Force Base, Ohio<br>Attn: WCACT<br>For: Capt. N. Munson, WCLPS, G. W. Sherman, WCLEE, WCOSI | 69 through 72 |
| 31. | Commanding Officer<br>Jet Propulsion Laboratory<br>Pasadena, California<br>Attn: W. H. Pickering, I. E. Newlan | 73 |
| 32. | Univ. of California Radiation Lab<br>Technical Information Division<br>P. O. Box 808, Livermore, California<br>Attn: Clovis G. Craig<br>For: Dr. Robert H. Fox | 74 |
| 33. | Los Alamos Scientific Laboratory<br>P. O. Box 1663<br>Los Alamos, New Mexico<br>Attn: Report Librarian<br>For: Dr. George M. Grover | 75 |
| 34. | Commander<br>Air Force Special Weapons Center<br>Technical Information & Intelligence Office<br>Kirtland Air Force Base, New Mexico<br>Attn: Kathleen P. Nolan | 76 |

## DISTRIBUTION LIST (Continued)

| | | Copy No. |
|---|---|---|
| 35. | School of Aviation Medicine<br>Brooks Air Force Base, Texas | 77 |
| 36. | Commander<br>Aero-space Technical Intelligence Center<br>Wright-Patterson Air Force Base, Ohio<br>Attn: H. Holzbauer, AFCIN-4 Bia | 78 |
| 37. | National Aeronautics & Space Administration<br>1512 H. Street, N. W., Washington 25, D. C.<br>Attn: Dr. Addison M. Rothrock | 79 through 83 |
| 38. | The Martin Company<br>P. O. Box 5042, Baltimore 20, Maryland<br>Attn: AEC Document Custodian | 86 through 90 |
| 39. | Advanced Research Project Agency<br>The Pentagon, 3D154, Washington 25, D. C.<br>Attn: Fred A. Koether or Donald E. Percy | 85 |

# FOREWORD

SNAP I is the first of a family of devices to convert nuclear energy to electrical for use in space. The SNAP Systems for Nuclear Auxiliary Power - programs are sponsored by the Atomic Energy Commission; the SNAP I prime contractor is The Martin Company. SNAP I was designed to utilize a radio isotope as the energy source.

The SNAP I Power Conversion System utilizes mercury as the working fluid for a Rankine cycle. A radioisotope is used as the energy source to vaporize mercury in a boiler; turbo-machinery extracts the useful energy from the vapor and converts it into electrical energy; the exhaust vapor is condensed by rejecting the waste thermal energy to space in a condenser-radiator.

During the SNAP I Power Conversion System development, Thompson Ramo Wooldridge has been responsible for the development of the following items:

Turbo-machinery

- Mercury vapor turbine
- Alternator
- Lubricant and condensate pump
- Mercury lubricated bearings

Speed Control

Condenser-Radiator

A series of eight Engineering Reports have been prepared describing Thompson Ramo Wooldridge's SNAP I Power Conversion System development program. These are as follows:

| | |
|---|---|
| ER-4050 | Systems |
| ER-4051 | Turbine |
| ER-4052 | Alternator |
| ER-4053 | Pump |
| ER-4054 | Bearings |
| ER-4055 | Control |
| ER-4056 | Condenser-Radiator |
| ER-4057 | Materials |

The material in this report deals specifically with the developmental history of the pump for the SNAP I Power Conversion System. This report is submitted as part of the requirements of Purchase Order OE-0101 from The Martin Company, issued under the Atomic Energy Commission prime contract AT(30-3)-217.

# TABLE OF CONTENTS

## 1.0 SUMMARY

The SNAP I mercury pump development program included the analysis, design, fabrication and testing of several types of pumps. Preliminary analysis and experimental testing indicated that a jet boosted-centrifugal pump directly coupled to the turbine shaft satisfied the SNAP I requirements. The final SNAP I mercury pump configuration consisted of a four vaned radial, open impeller supplemented by a liquid mercury jet boost stage. Primary design considerations were reliability, simplicity and minimum weight. Analytical and empirical jet-centrifugal design procedures were evolved and verified by experimental testing for low specific speed, cavitation limited, small size, liquid mercury pumps.

Experimental results verified that the jet-centrifugal mercury pump performance exceeded system design specifications. The final design point requirements for outlet pressure and efficiency were 287 psia and 20%, respectively. This compares to achieved performance of 380 psi developed head with an efficiency of 27% at design speed and inlet pressure.

The final jet-centrifugal pump was successfully incorporated for pump-bearing subsystem tests and final system integration and tests. The SNAP I power conversion system exceeded the design 60 day life in a system endurance test. The system accumulated 2510 hours of endurance testing with satisfactory operation.

## 2.0 INTRODUCTION

Figure 2-1 shows the turbo-machinery package of SNAP I--the first space powerplant. This unique subminiature electric power generator contains the turbine, alternator, and condensate pump for the Rankine cycle power conversion system. These components are mounted on a common shaft rotating at 40,000 rpm and supported by mercury lubricated bearings.

Required to operate unattended for long durations in stringent environments, the SNAP I turbo-machinery package is the result of advanced engineering concepts in analysis, design, fabrication, and experimentation. The SNAP I mercury pump is required to operate at high speeds and produce a high head with low flow and a very low inlet pressure for long periods of unattended operation. Considerations of cavitation, small size, low specific speed, high fluid density, and the required extrapolation of empirical pump design constants indicate that the state-of-the-art in pump design has been significantly advanced by the successful attainment of these requirements.

The SNAP I pump development program was established to determine feasibility, correlate analytical and experimental results, and develop a pump capable of meeting system design specifications. This report describes the efforts that resulted in a successful SNAP I mercury pump.

SNAP I TURBOMACHINERY PACKAGE

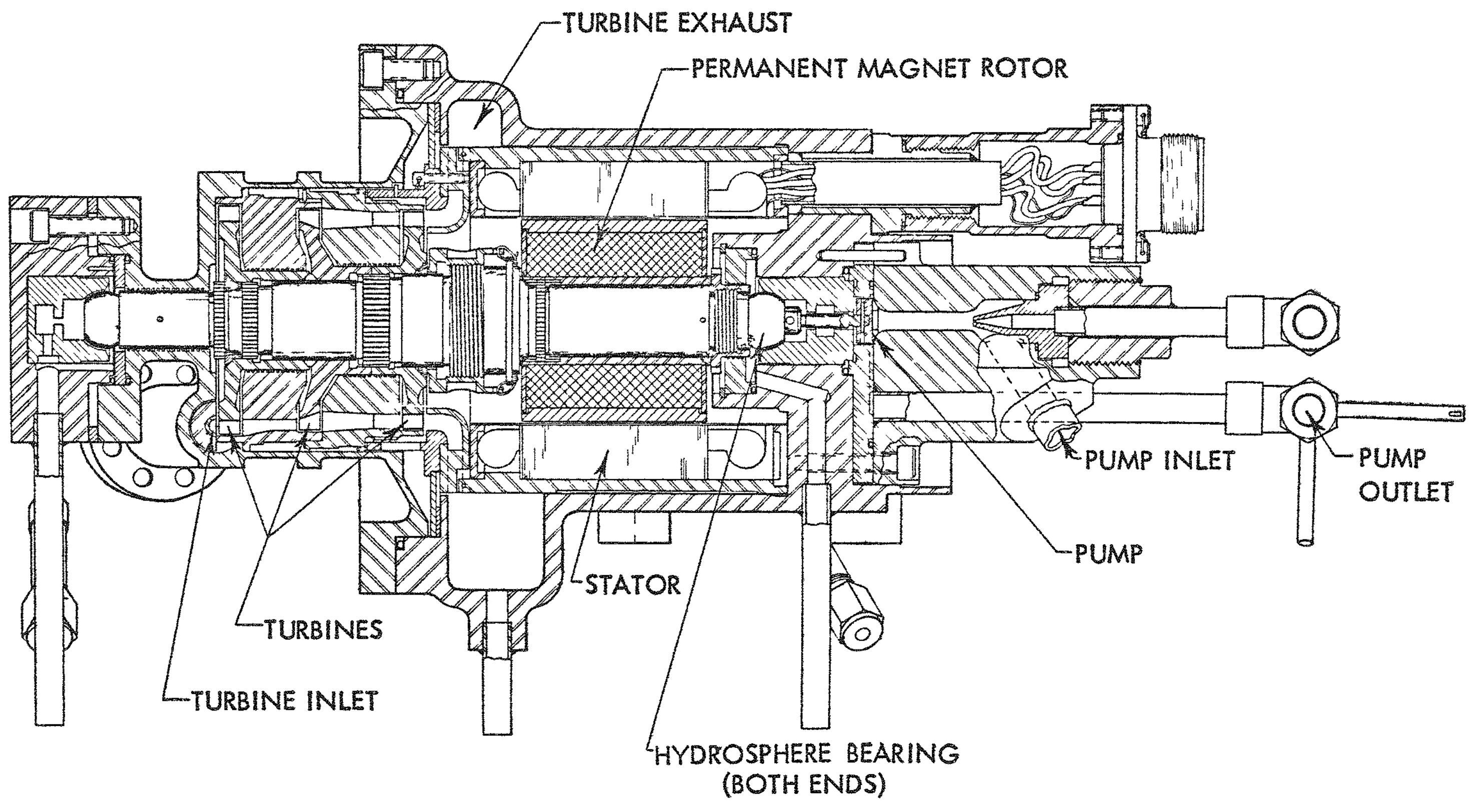


FIGURE 2-1

# 3.0 PUMP DESIGN

## 3.1 Pump Specifications and Requirements

The Rankine cycle power conversion system turbine requires high pressure, high temperature vapor. The heat content of the vapor is supplied by the boiler, but a feed pump is required to deliver the fluid from the condenser to the boiler at the desired pressure and flow rate. The pressure at the pump outlet must be greater than the turbine inlet pressure by an amount equal to the frictional pressure drop in the boiler lines and the pressure drop in any pressure control element through which the high pressure fluid may flow.

The pump for the SNAP I power conversion system is required to pump the low pressure mercury from the subcooler and continuously supply the boiler with high pressure working fluid and the turbo-machinery bearings with high pressure lubricant (see Figure 3-1). The pump must fulfill this requirement with no external leakage and minimum weight. The specific pump design objectives changed during the course of the development program because of increased system power output requirements and as the bearing flow requirements became more firmly established. It was necessary to change the design concept as some of the early pump designs were incapable of keeping pace with the increasing flow requirements. This overall system development resulted finally in the specific design requirements listed in Table 3-1.

The pump design approach had to be changed to meet these changing requirements and, although this involved investigation of several pump types, the general design considerations, discussed below, remained unchanged.

### 3.1.1 Reliability

Reliability is the prime design consideration since the pump is required to operate continuously and unattended for at least 60 days. This criterion emphasizes the need for the selection of a design with a minimum number of moving parts subject to wear, fatigue, or seizing.

### 3.1.2 Weight

The weight of the pump must be kept to a minimum because of the high weight penalty assigned to orbital operation. A heavier design could only be accepted if a greater degree of reliability or performance could be obtained.

### 3.1.3 Efficiency and Performance

The attainment of optimum pump efficiency is a secondary design consideration, since pumping power is relatively low compared with the turbine shaft power output. The pump performance must be satisfactory to supply the required flow and pressure with a reasonable pump overall efficiency.

SNAP I POWER CONVERSION SYSTEM FLOW SCHEMATIC

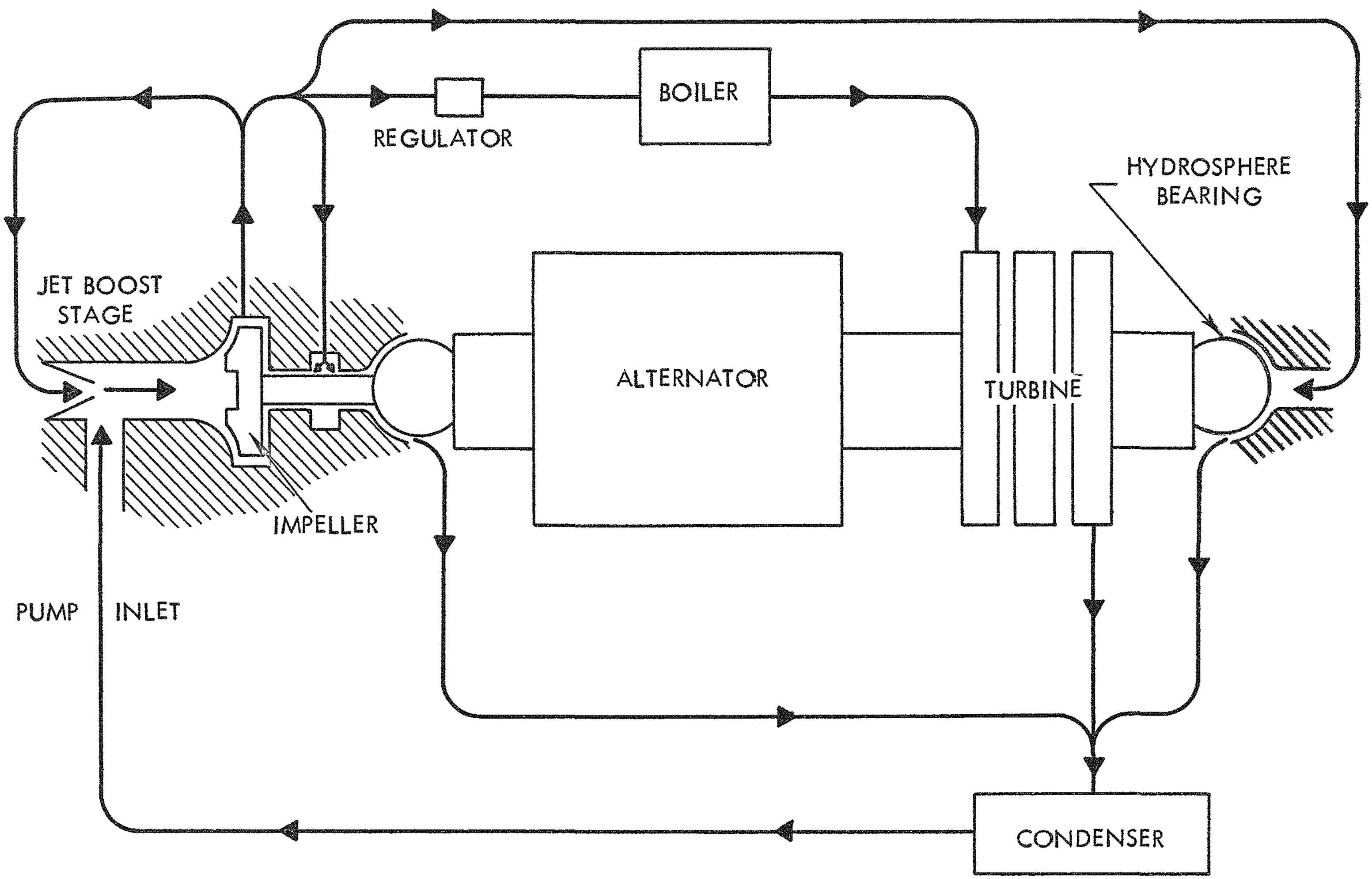


FIGURE 3-1

TABLE 3-1

SNAP I PUMP REQUIREMENTS

| | |
|---|---|
| Fluid | Liquid Hg |
| Shaft speed - rpm | 40,000 |
| Discharge pressure - psia | 287 |
| Net developed head-ft | 50 |
| Inlet pressure - psia | 1.86 |
| Inlet temperature - $^{o}F$ | 330 |
| Design capacity - lb/min | 12 |
| GPM | .1091 |
| Power limit (max) - watts | 100 |
| Life - days | 60 |
| Impeller specific speed | 705 |
| $\sigma$ = NPSH/H | .006 |

### 3.1.4 Cavitation

Cavitation is seriously detrimental to pump operation since it reduces performance and efficiency and may cause severe pump damage which impairs reliability and performance considerably. The occurrence of cavitation depends on the effects of eye diameter, amount of prerotation, net positive suction head (NPSH), rotational speed, manufacturing deviations, and surface roughnesses. Any flow abnormalities can further limit cavitation-free operation. Considerable care must be exercised to reduce cavitation effects to a minimum and maintain performance and reliability at a high level.

### 3.1.5 Leakage

External leakage from the system must be zero since the use of a makeup feed system imposes a high weight penalty and definitely limits the life of the system.

### 3.1.6 Life

The minimum life of the pump is 60 days of continuous unattended operation.

### 3.1.7 System Integration

The effect of the pump configuration and characteristics on the system must be evaluated and matched in order to provide optimum pump performance. Specific areas of evaluation are:

a. Power required to drive pump.
b. Axial and radial thrust loads resulting from the pump.
c. Fabrication and assembly of pump parts.

## 3.2 Pump Selection

There are three sources of power available to drive the pump:

a. High temperature mercury vapor.
b. Electrical power from the alternator.
c. The turbo-alternator shaft.

### 3.2.1 Vapor Driven Pumps

High temperature mercury vapor could be used to drive a vapor jet pump, a piston pump, or an auxiliary turbine. The vapor jet pump is simple and reliable, but its efficiency is very low (3 to 4%). The vapor jet pump is applicable to processes where heating in addition to pumping is desirable, but in this system a temperature rise is undesirable due to the requirement to recirculate the bearing lubricant. A high temperature vapor motor requires extensive development and still exhibits doubtful reliability due to the high temperature valving. An auxiliary turbine provides a good drive, but it introduces the complexities of an additional rotating unit.

3.2.2 Electrically Driven Pumps

The use of electrical energy for driving the pumps has the advantage of making it possible to start the pump and the system by means of external power supply and of simplifying the control system. Pumping problems are minimized, but the addition of a hermetically sealed unit introduces new problems, such as weight, sealing of electrical components from working fluid, cooling, and lubrication. Reliability is also reduced with the addition of a second set of rotating components.

Due to the magnetic properties of the liquid metal mercury, the electrical energy could also power an electromagnetic pump, although an electromagnetic pump to deliver the required head and flow would be very heavy and the efficiency would be extremely low ( $\approx$ 2%).

3.2.3 Shaft Driven Pumps

The use of the turbo-alternator package shaft to drive the pump simplifies the leakage problem, increases reliability by reducing the number of moving parts, and increases the efficiency of the power conversion system by eliminating a second rotating unit with a motor or turbine drive and a separate set of bearings. For these reasons the effort was confined to the evaluation of several pump types which may be mounted on the turbo-alternator shaft.

3.2.3.1 Piston Pump

Piston type pumps appear advantageous from the standpoint of cavitation, startup, and control, but the problems encountered in obtaining a suitable high speed drive and valving appear to offset any gain in performance and control. In order to drive directly from the main shaft, a cam or slight eccentric, which increases wear and lubrication problems, is required. If the piston pump is driven at a low enough speed to incorporate reliable valving, a separate drive or gearing is required and the weight increases considerably. The mechanical and/or fluid dynamics problems encountered in a piston pump design are unduly severe.

3.2.3.2 Gear Pumps and Other Rotating Positive Displacement Pumps

These pumps have relatively high net positive suction head requirements which practically eliminate them from consideration. In addition, if driven at 40,000 rpm, dynamics and wear problems develop on the gears and other moving parts and lower the mechanical efficiency.

3.2.3.3 Diaphragm Pumps

Diaphragm pumps present much the same difficulties as piston type pumps. They have the added disadvantage of doubtful reliability for the life required in this application.

3.2.3.4 Centrifugal Pumps

Centrifugal pumps present the problem of introducing the inlet flow at only 1.7 psi above the saturation pressure into a 40,000 rpm impeller without causing cavitation. But centrifugal pumps are advantageous from the standpoint of simplicity, size, external leakage control, and reliability. Because of these inherent capabilities it was decided to develop a centrifugal pump to be mounted directly on the turbo-alternator shaft.

3.3 Pump Parameters and Design Considerations

Every centrifugal pump consists of two principal parts: an impeller, which forces the liquid into a rotary motion by impelling action, and the pump housing, which directs the liquid to the impeller and leads it away under higher pressure. In standard centrifugal pump design practice, the term used to describe the impeller and housing configuration is specific speed ($N_s$). This term categorizes the pump and is used as the basis for all important design and performance information. With each specific speed is associated definite proportions of impeller and housing to obtain maximum efficiency at design point. Specific speed is defined as follows:

$$N_s = \frac{N\sqrt{Q}}{H^{3/4}} \tag{1}$$

where N = speed in rpm

Q = capacity in gpm

H = net developed head in ft

Also, to obtain a relationship between the static developed head and speed,

$$H = \frac{K(u_2^2 - u_1^2)}{2g} \tag{2}$$

where $u_1$ and $u_2$ = peripheral velocity of the impeller at ID and OD of blades

g = gravitational constant

K = a coefficient which depends on blade angle, specific speed, and number of vanes. (Values of this coefficient are normally determined experimentally from water pump tests and plotted versus specific speed for design use).

It is apparent from these centrifugal pump relationships that low specific speed pumps are normally used for high speed and small volume flow applications and thus require a large diameter and small flow passages. However, in the SNAP I requirements two other considerations enter the analysis, i.e., the high speed as determined by other requirements and the high density of mercury. Thus, the requirements call for the performance of a low specific speed pump design utilizing a high shaft speed and extremely small flow passages. Both of these factors combine to limit the pump diameter to subminiature size where fabrication of normal configurations approaches impractical or impossible conditions. Also, the small volume of the passages requires that extremely close clearances be maintained to prevent excessive internal leakage.

Also included in pump sizing considerations is the value of available NPSH (net positive suction head). The available NPSH for the pumping application is

$$NPSH = h_a + h_s - h_v - h_l \qquad (3)$$

where

$h_a$ = the absolute pressure in the condenser (as determined by the Rankine cycle).

$h_s$ = the static head above pump centerline (in the SNAP I application, no static head will prevail due to the zero gravity environment).

$h_v$ = the vapor pressure at pump inlet temperature.

$h_l$ = the head loss in the inlet passages, subcooler and condenser, (note that this is the only term in the NPSH which can be controlled in the pump design).

However, cavitation will start in a centrifugal pump when the available NPSH is equal to the velocity head combined with the dynamic depression in the impeller eye. Thus, to insure reliable operation the minimum NPSH should be

$$NPSH = \frac{c_1^2}{2g} + \lambda \frac{w_1^2}{2g} \qquad (4)$$

where

$c_1$ and $w_1$ = the average absolute and relative velocities respectively through the impeller eye.

$\lambda$ = experimental dynamic depression coefficient.

Although the coefficient $\lambda$ is difficult to determine, it can be seen from the parameters of equations (3) and (4) that the pump design must carefully control the impeller approach and eye dimensions. To obtain a minimum loss from each quantity, there should be a small inlet diameter for dynamic depression, but yet large enough to keep the inlet velocity head loss at a low value and to minimize the forced vortex, or prerotation. The terms must be optimized with geometric considerations to produce a minimum suction head requirement.

Cavitation is generally described by an experimental cavitation coefficient $\sigma$. This coefficient is defined as

$$\sigma = \frac{NPSH}{H} \tag{5}$$

where

NPSH = the net positive suction head at any operating point.

H = the net developed head at the same point.

Since all design factors governing cavitation (eye area, number of vanes, etc.) are continuous functions of specific speed, $\sigma$ has a definite relationship with $N_s$. Obtained values of $\sigma$ at which incipient cavitation begins are plotted on Figure 3-2 for standard pumps as published by the Hydraulic Institute. Normally, operating values below those shown in Figure 3-2 indicate that the pump is operating under conditions which allow cavitation to develop to a serious degree. Comparison of these values and the values listed in Table 3-1 shows that SNAP I requirements are well beyond the range of standard pumps. However, the $\sigma$ value can be improved by the use of a boost stage ahead of the main impeller stage. Also, an oversized pump (large diameter) is sometimes used to meet specified capacity when operating under cavitating conditions.

Another cavitation correlating parameter which has been widely adopted in pump testing is suction specific speed, $N_{sv}$, which is defined as follows:

$$N_{sv} = \frac{N \sqrt{Q}}{(NPSH)^{.75}}$$

The development of this equation is based on the use of similarity relations (affinity laws) at conditions approaching cavitation. With special designs, suction specific speeds approaching 15,000 have been obtained for single suction pumps at the best efficiency point. Higher values of suction specific speed have been obtained with an axial-flow booster impeller or an ejector ahead of the regular impeller entrance.

The major SNAP I pump design considerations may be summarized as follows:

CAVITATION CONSTANT VERSUS SPECIFIC SPEED

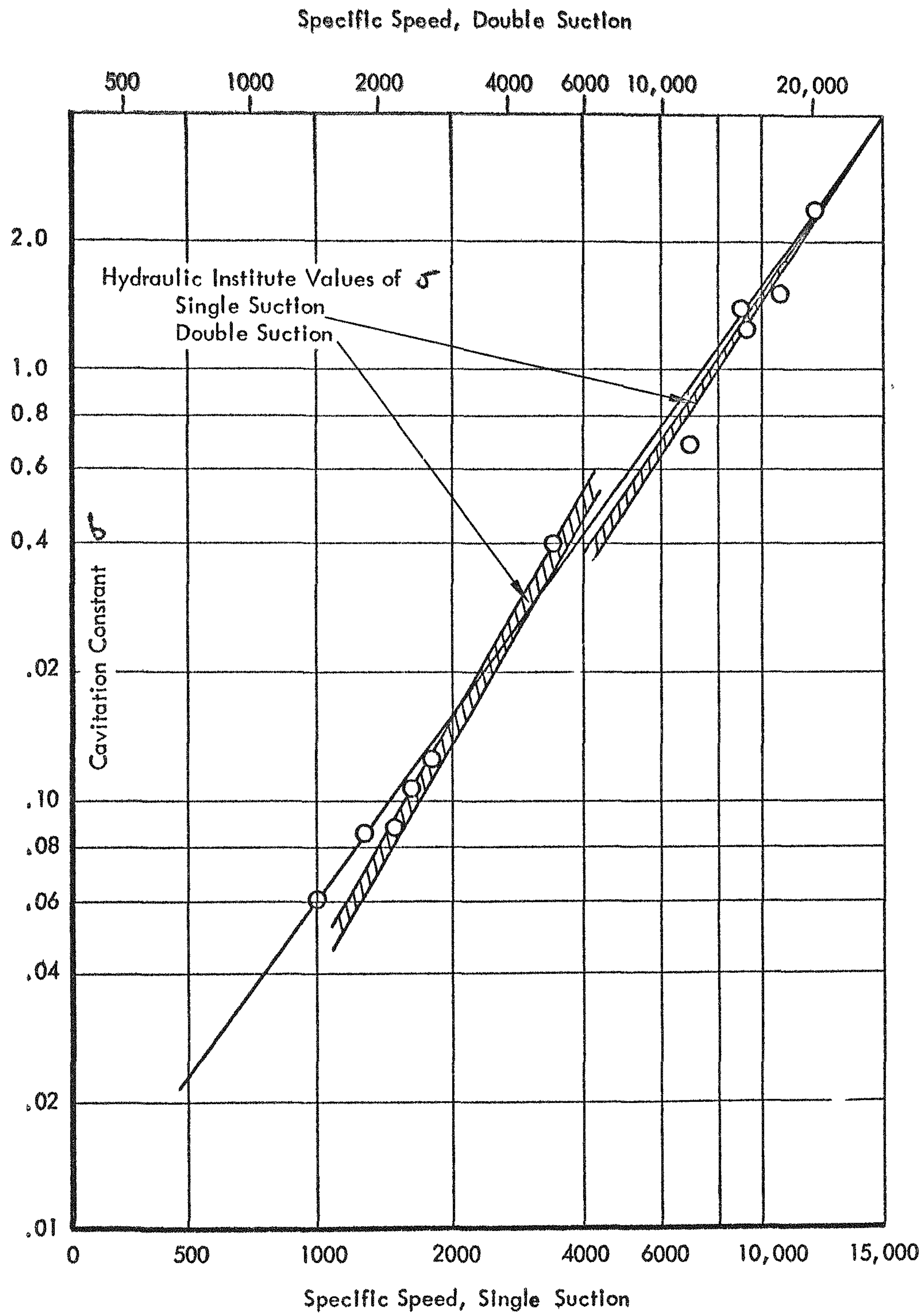


FIGURE 3-2

1. Reliability, simplicity, and weight optimization are of prime importance.

2. Although most passages in the impeller and housing require extensive analysis to determine the velocity and pressure distributions, a majority of the calculations can be made by assuming average velocity and pressure conditions.

3. The mercury pump design constants associated with specific speed can be, at best, only extrapolated from standard design data for water pumps. However, fluid density and pump speed must also be considered in the use of specific speed.

4. Ample suction approach area without excessive prerotation and also streamlining of the impeller approach are essential to obtain optimum cavitation characteristics.

5. Boost staging or an oversized cavitating pump or both must be considered to meet specified capacity and inlet pressure.

## 4.0 PRELIMINARY PUMP DEVELOPMENT

A pump development program was established to determine feasibility, correlate analytical and experimental results, and develop a pump capable of meeting system design specifications. A preliminary literature search was conducted to determine the state-of-the-art of pump development. This survey indicated that cavitation and miniaturization would be severe problem areas. Cavitation must be avoided in order to provide for long-term, reliable, pump operation. However, the occurrence of cavitation has not been defined adequately either analytically or experimentally. The small size of pump required in this application indicated that severe fabrication and design limitations would exist. The validity of extrapolation from empirical pump design constants for normal pumps (100 gpm or more) to very small pumps (less than .15 gpm) was extremely doubtful.

The specific objectives of the pump development program were as follows:

1. Determine feasibility of high speed, low flow, liquid mercury pumps.
2. Obtain experimental relationships of head, power, and efficiency versus flow.
3. Determine inlet pressure (NPSH) requirements (cavitation curves).
4. Obtain performance versus speed relationships.
5. Evaluate geometry effect on performance (front-face clearance, jet nozzle spacing, etc.)
6. Determine pump operating characteristics such as startup ability, pressure fluctuations, system integration, etc.

Variations of three basic designs composed the major portion of the SNAP I pump development. These three were the shaft pump, the slinger pump, and the vaned impeller pump. Figure 4-1 is a hardware composite photograph and Figure 4-9 is a comparison of performance of all the pump types. A brief history of each pump will now be presented chronologically.

### 4.1 Shaft Pump

For simplicity purposes and because of the desire for no shaft overhang at the bearings, the first type of pump investigated was the shaft pump utilizing one or two radial holes in the shaft to impel the fluid as shown in Figure 4-2. It is essentially a one blade centrifugal pump with a 90° inlet and outlet blade angle. Design analysis was based on Euler's equation for developed head with the assumption that the fluid particles obtain the peripheral velocity of the shaft. Since the initial flow requirement was quite low,

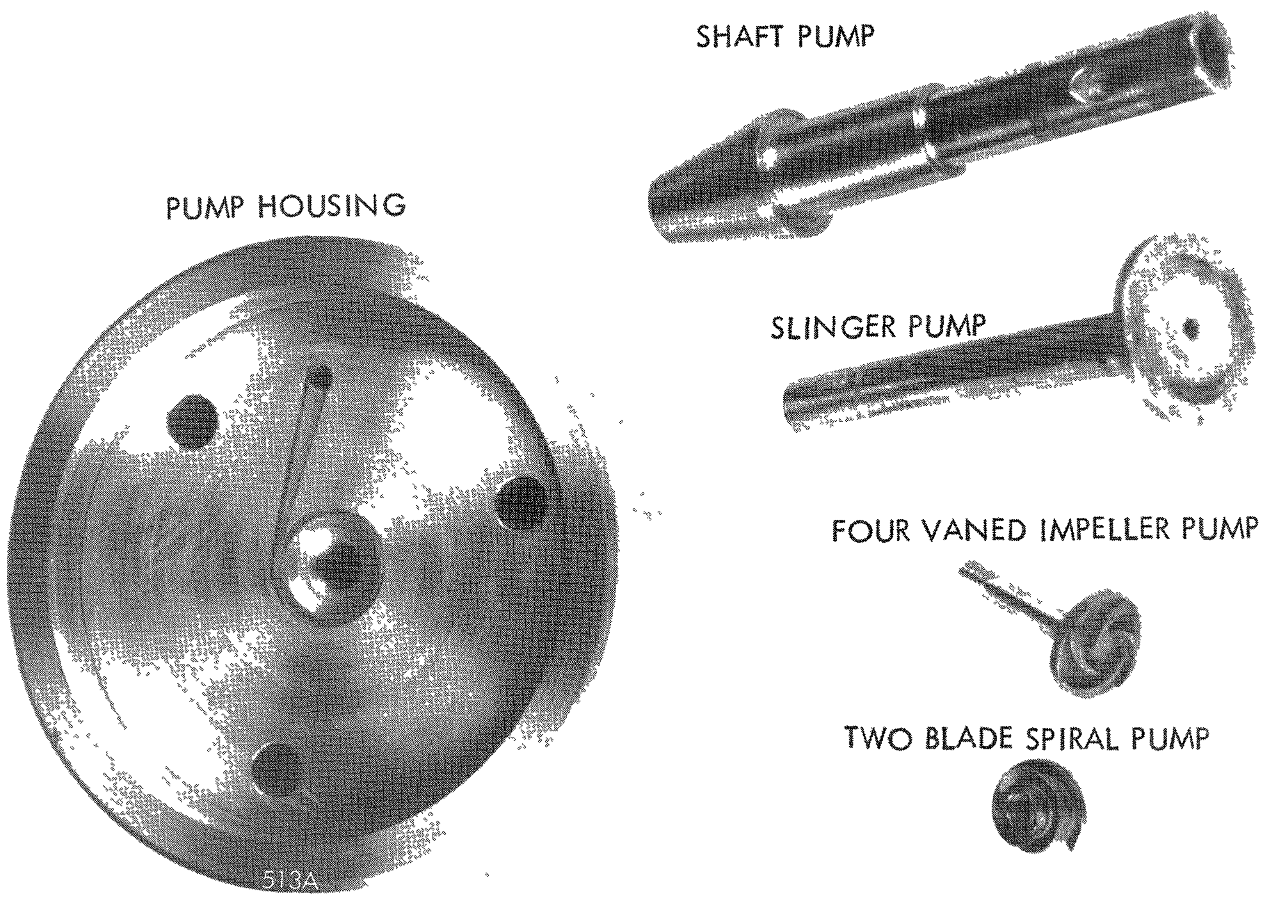


PUMP HARDWARE

FIGURE 4-1

SHAFT PUMP TEST ASSEMBLY

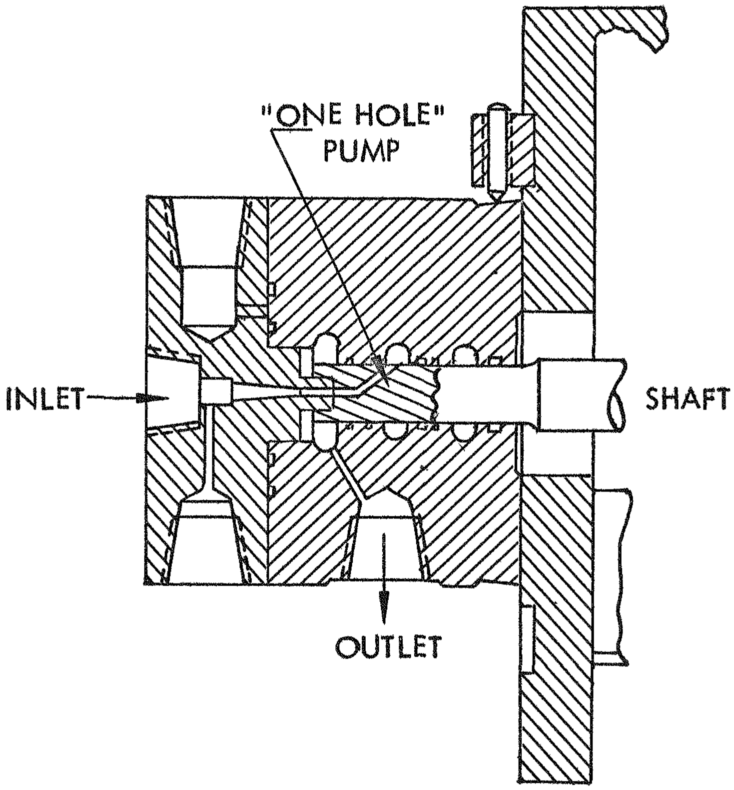


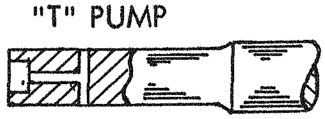


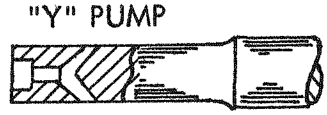


FIGURE 4-2

the need for highly streamlined passages and shockless entry was not critical. Several variations of a .3 inch diameter shaft pump were built and tested. The "T" configuration pump developed heads up to 12 feet of mercury (70 psi) at a flow rate of 5 lb/min at approximately 12 psia inlet pressure. The best performance of the "Y" pump showed a developed head of 15 feet of mercury (88 psi) at 6 lb/min. Figure 4-9 shows the performance of the "one-hole" pump which was the most successful of the shaft pumps. However, its performance of 155 psia at 8 lb/min fell off sharply at reduced inlet pressures as was characteristic of all of the shaft pumps.

Thus it can be concluded that although the shaft pump was the simplest configuration for the early SNAP I requirements, the lack of adequate flow passages and of shockless entry definitely limited the capacity.

## 4.2 Slinger Pump

As was mentioned previously, the characteristically low specific speed of the SNAP I pumps indicates very small impeller flow passages while shaft speed requires a small diameter. These considerations are valid for a vaned impeller; however, if the vanes are not used the fluid is not guided and pumping is accomplished by viscous drag. Thus, by eliminating the impeller flow passages the diameter must be increased to compensate for the accompanying fluid "slip" caused by the loss of guidance of impelling surfaces. Actually, the slinger or disk pump might be viewed as the general configuration required at the extreme low end of the specific speed range where blade heights are infinitesimally small and impeller diameter is very large.

The slinger type pump has the advantages of simplicity in construction, durability, and it allows a reasonable inlet configuration. The design of the slinger or disk pump was based on the assumption of the generation of head by forced vortex theory with the analysis of losses based on theoretical and experimental relationships for viscous drag of a disk in a housing.

A slinger pump was designed and tested (see Figure 4-9) to determine the feasibility of a disk pump using a relatively simple (circular volute) housing. As was expected, power consumption was very high due to disk friction; and although the hydraulic performance could be improved by a redesign, the low efficiency and high power consumption clearly showed that a vaneless pump was not attractive for the SNAP I system.

## 4.3 Four-Vaned Impeller Pump

As SNAP I system head and flow requirements increased, a configuration based on standard centrifugal pump design practice was considered. Bearing development and system package studies indicated that an overhung pump could be incorporated.

The design of the impeller and volute was based primarily on the standard methods suggested for large pumps and modified to overcome the limited NPSH available. Two different vane configurations with a .4 inch diameter radial flow impeller were investigated. The difference in the two vane configurations, designated S/N 1 and S/N 2, was that S/N 1 had an inlet angle of 6° which was 1-1/2° larger than that of S/N 2. A photograph of the S/N 1 impeller, Figure 4-3, shows that the leading edge of the vane is a continuous curve determined by the inlet and discharge angles. In order to obtain a thin vane section at the inlet for shockless entry, and yet have a substantial blade for strength and erosion considerations, a variable thickness vane was used.

Performance of the two impeller configurations was obtained by testing in the general arrangement shown in Figure 4-4 and is shown graphically in Figure 4-5. The S/N 2 impeller performance was the better of the two because its geometry results in a higher average outlet angle which causes an increase in the tangential component of the absolute outlet velocity. Since the outlet velocity is converted into head, the higher outlet velocity results in increased developed head.

Development testing of the vaned impeller determined the effects of various pump parameters on performance. Performance versus speed data, plotted in Figure 4-6, showed that head, capacity, and power consumption closely follow the basic centrifugal pump relationships. These affinity laws state: when speed is changed, capacity varies directly as the speed, the head varies directly as the square of speed, and power consumption varies directly as the cube of the speed. Another major parameter was impeller front face clearance. Since practical manufacturing considerations required an open impeller design, the internal leakage was from the front side to the back side of the impeller vanes. Thus, instead of using close clearance wear rings to minimize leakage, as in shrouded impellers, the front face clearance must be closely controlled to minimize leakage.

The best performance of the four-vaned impeller pump at design inlet pressure is shown in Figure 4-9.

Performance at various pump inlet pressures was investigated and indicated that design head and capacity were not obtained through the use of the oversized impeller. However, with a small increase in pump inlet pressure, the required performance could be obtained. This suggested the incorporation of a boost stage for the vaned impeller.

During most of the component testing, straight radial vanes were used on the back face of the impeller to prevent leakage out the back of the housing. For most operating conditions the back vanes provided a seal by pumping the fluid on the back face in order to establish a free liquid surface. Also, a majority of the data was obtained at room temperature since it was found that design temperature operation affected performance primarily due to thermal expansion of the pump and housing rather than changing fluid properties.

### 4.4 Two-Blade Spiral Pump

The design of the four-vaned impeller was paralleled by the design of a 0.4 inch diameter two-blade spiral pump, shown in Figure 4-7. Although the configuration is that of a mixed

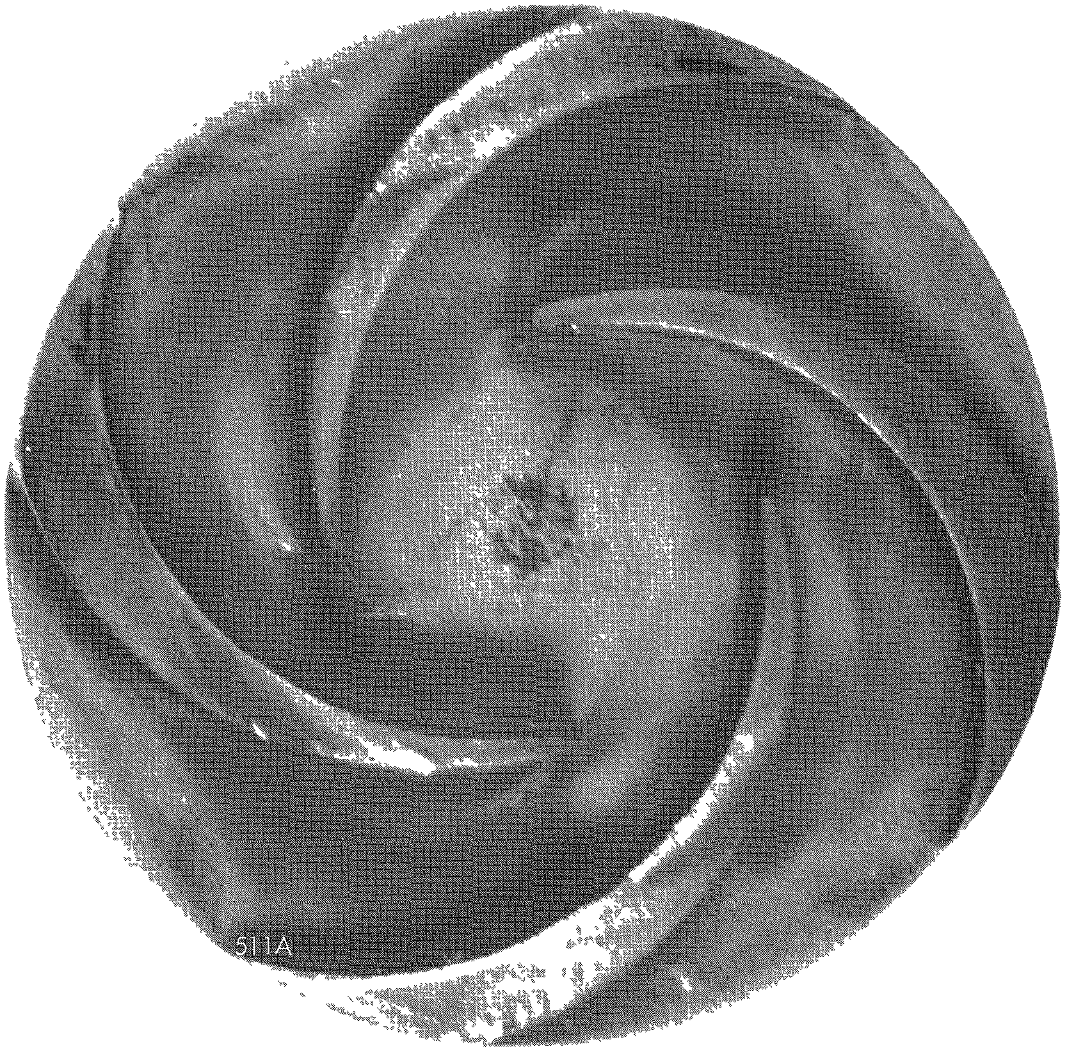


FOUR VANED IMPELLER PUMP



FIGURE 4-3

FOUR VANED IMPELLER TEST ASSEMBLY

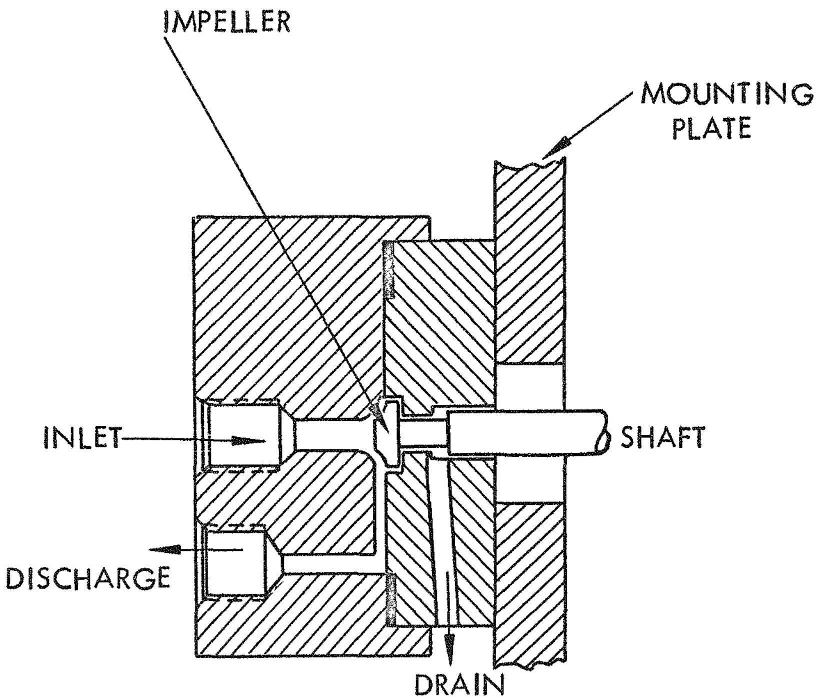


FIGURE 4-4

EFFECT OF GEOMETRY ON IMPELLER PERFORMANCE

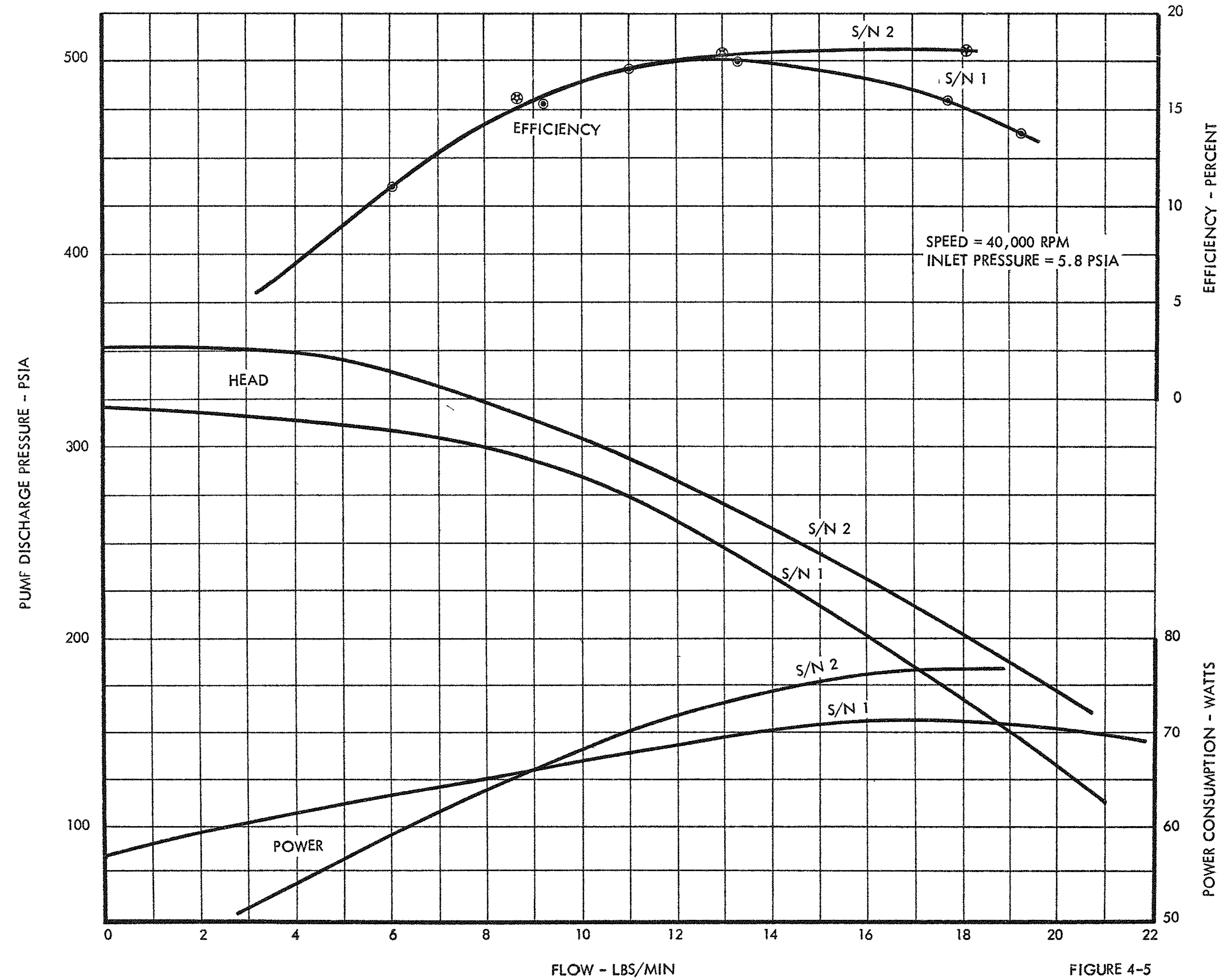


FIGURE 4-5

IMPELLER PERFORMANCE VERSUS SPEED

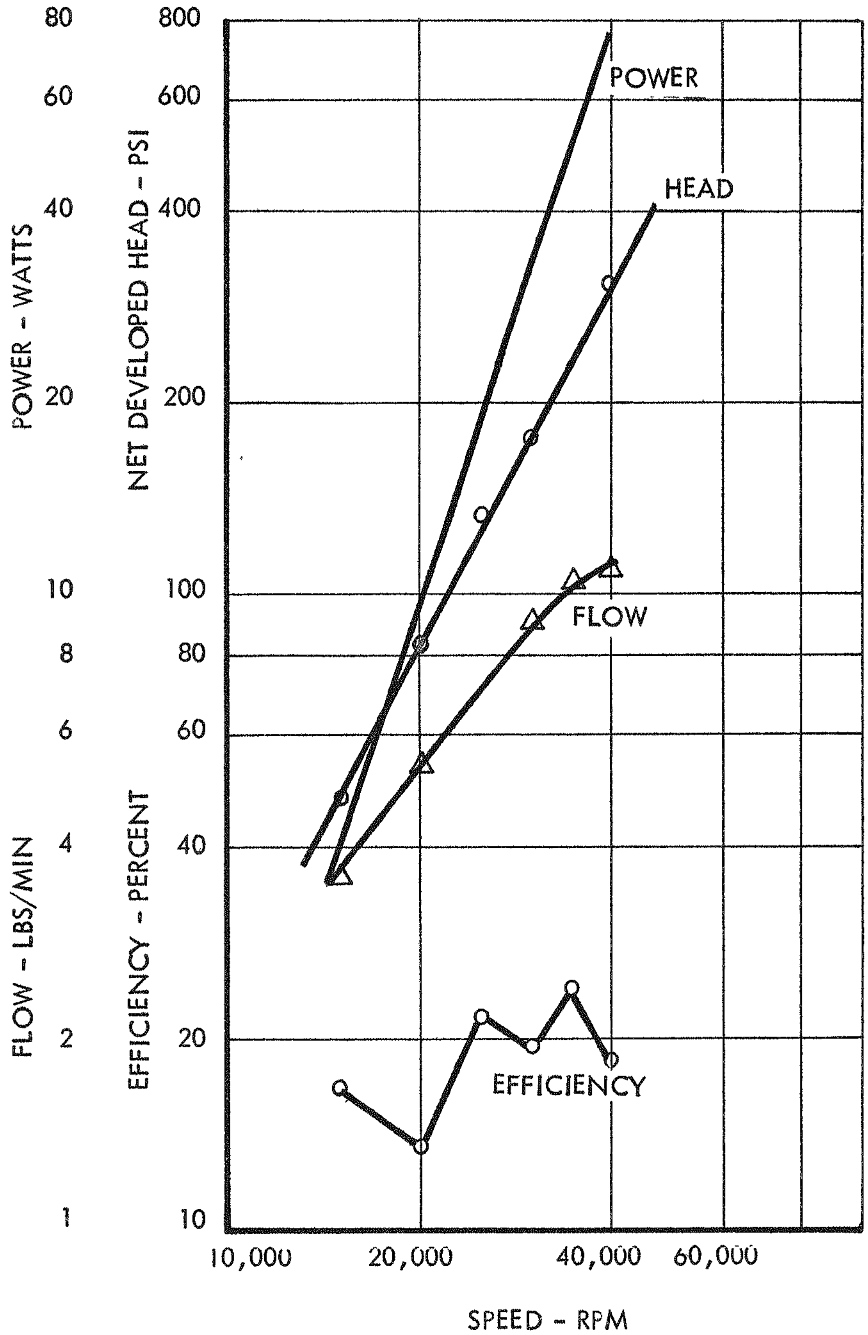


FIGURE 4-6


TWO BLADE SPIRAL PUMP

FIGURE 4-7

flow pump with impeller proportions of a high specific speed pump (4000 to 8000), the design allowed a large inlet passage and a minimum change in fluid direction through the impeller.

Performance of the two-blade spiral pump at design inlet pressure is shown in Figure 4-9. Since all the fluid particles do not obtain the peripheral velocity of the impeller outside diameter, the resultant tangential component of the absolute outlet velocity is an average of the velocities across the discharge passage. Thus, a lower discharge pressure is expected for the mixed flow pump than for the same diameter radial flow four-vaned impeller. The characteristic head vs flow curve is slightly flatter than the other pumps tested and reached a capacity limit at approximately 8 lb/min where performance became unstable.

Although improved manufacturing quality, i.e., surface finish and dimensional accuracy, plus eye streamlining and improved sealing would increase performance, further development of the two blade spiral pump was discontinued because of the better performance of the radial flow type pump.

4.5 Jet-Centrifugal Pump

As was mentioned previously, the test results of the four vaned radial impeller indicated that a boost stage was necessary to obtain required capacity at design inlet pressure since the pump was operating under cavitating conditions. The most simple and practical boost configuration appeared to be a jet which could be mounted at the impeller inlet (see Figure 4-8). Design of the jet stage was based on a method which utilizes the conservation of momentum at the best efficiency point. Several nozzles were fabricated and tested at various nozzle to throat spacings. The original jet-centrifugal pump system used the alternator mercury coolant flow as the driving fluid. This method placed no increased demand upon the impeller stage since the alternator coolant flow was part of the system useful flow and was throttled to condenser pressure after passing through the alternator. Thus, the centrifugal stage did not require resizing. Optimization of the jet stage for these conditions resulted in a .014 inch nozzle diameter.

A final system revision which eliminated the need for alternator coolant flow necessitated a jet pump redesign to utilize full pump discharge pressure rather than the coolant flow pressure after losses through the alternator. Fortunately, the system useful flow requirements were reduced which meant that the impeller flow (now including recirculating jet flow) was approximately the same as that originally required in the four-vaned impeller development. The redesigned jet resulted in a .012 inch diameter nozzle. Thus, this jet boost stage combined with the S/N 1 four-vaned radial impeller represents the final component development configuration for the SNAP I pumping requirements. The S/N 1 impeller was selected because the higher head developed by the S/N 2 impeller was not necessary when utilizing the jet boost stage. Final testing included tests in the pump test rig, the bearing test rig, and the final SNAP I system package.

Overall jet-centrifugal pump characteristics are shown in Figure 4-9 at approximately .003 inch front face clearance. It is seen that cavitating performance was eliminated,

JET CENTRIFUGAL PUMP TEST ASSEMBLY

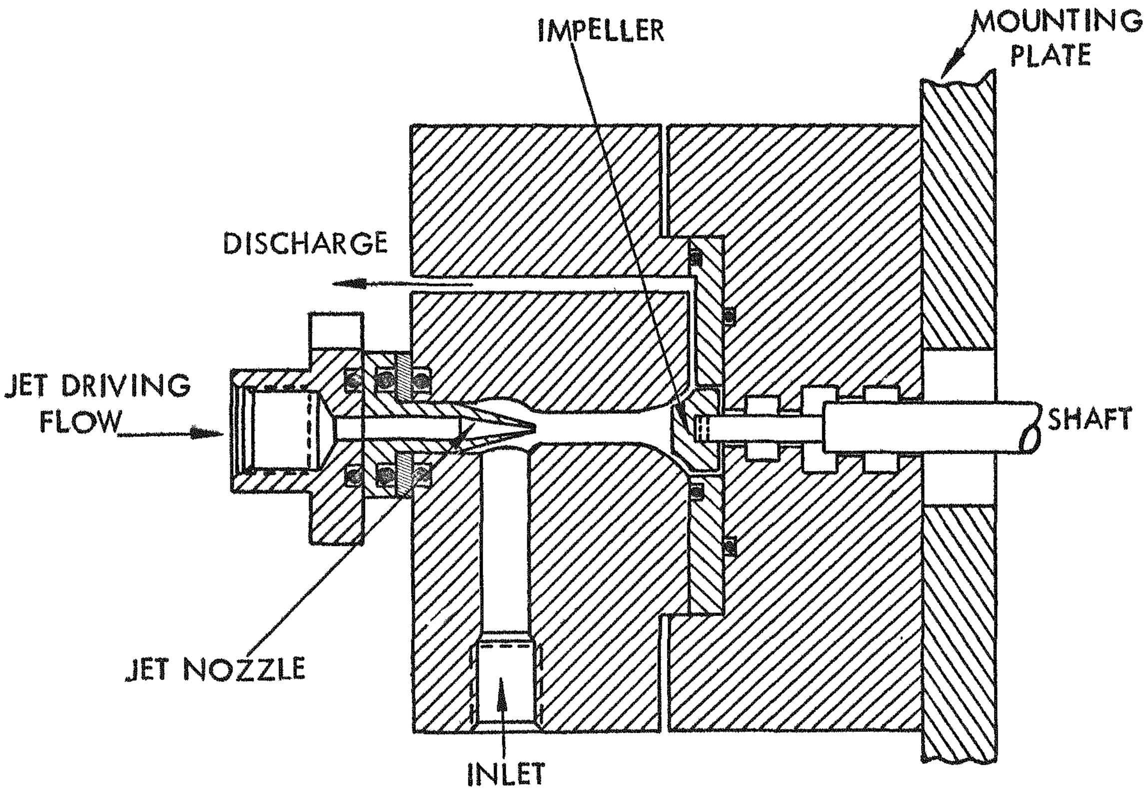


FIGURE 4-8

PUMP CHARACTERISTIC CURVES

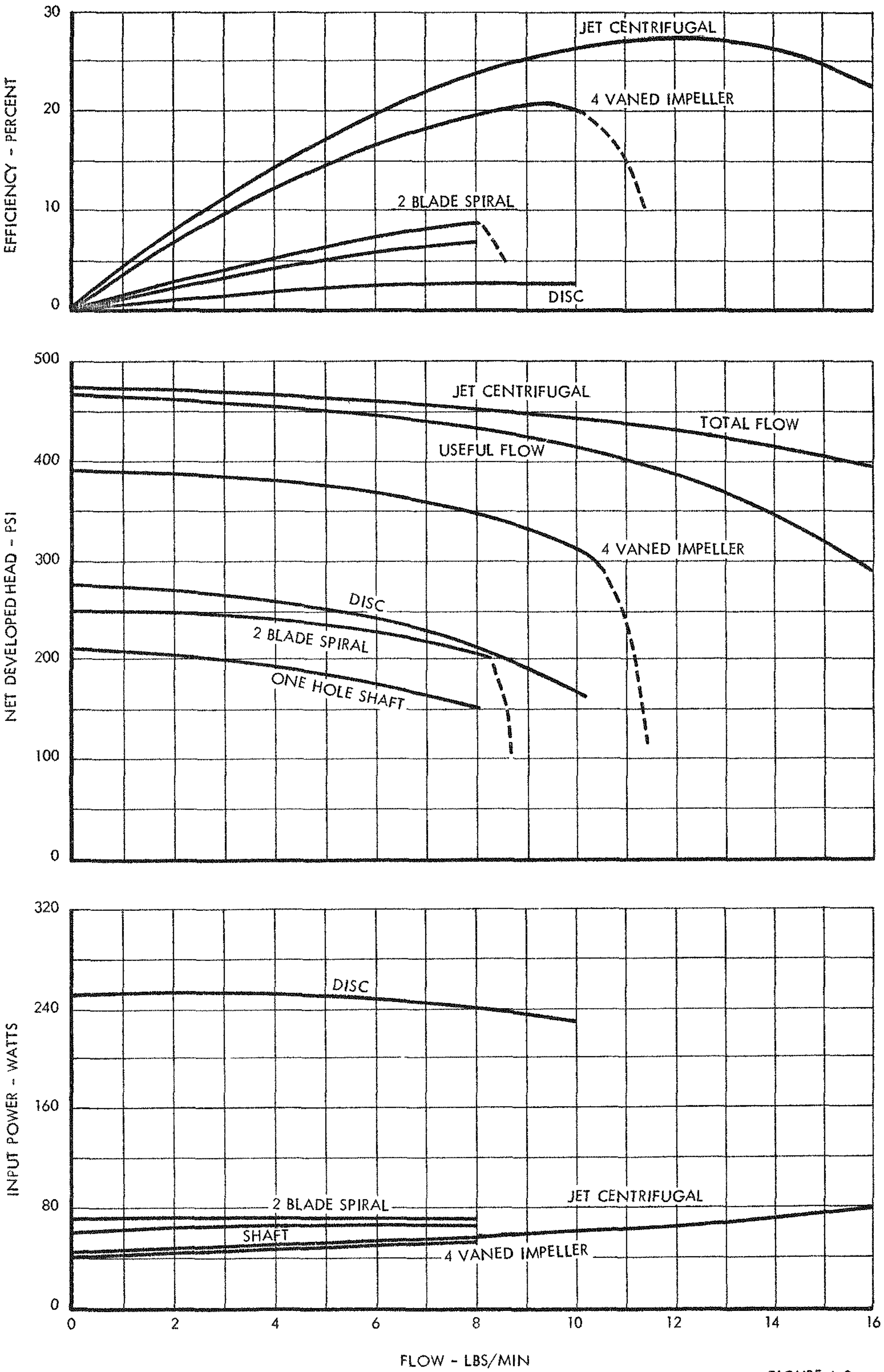


FIGURE 4-9

resulting in a high level of pump output. The recirculating flow includes both jet driving flow and leakage flow from the bearing supply.

A more detailed discussion of the SNAP I jet-centrifugal pump testing and results will be presented later.

## 5.0 JET-CENTRIFUGAL PUMP DEVELOPMENT

The experience gained from the preliminary SNAP I pump development program indicated that it was possible to design a pump to operate at very low inlet pressures. The test data also indicated that a jet pump was needed to raise the impeller inlet pressure to a value high enough to eliminate cavitation. Figure 4-9 shows a comparison of the SNAP I four-vaned impeller operation with and without a jet pump, and indicates very clearly the overall improvement in performance provided by the jet pump.

### 5.1 Jet-Centrifugal Pump Design Procedure

The SNAP I liquid mercury pump was designed using empirical methods and design constants for large centrifugal pumps as a guide, and modifying the analysis and design to incorporate the experimental test results from the SNAP I Development Program. The principal problem areas in extrapolating the empirical design constants for normal centrifugal pumps to the SNAP I pump are as follows:

1. High density of the liquid mercury.
2. High shaft speed - 40,000 rpm
3. Small size - .4 inch dia.
4. Low Flow - $<$.15 gpm
5. Low NPSH available

The design of the jet-centrifugal combination is based on the optimization of the jet boost stage and the impeller configuration to provide the system requirements.

#### 5.1.1 Impeller Design

A radial centrifugal impeller was designed for the SNAP I Pump based on the method for normal centrifugal pumps with modifications to incorporate the experimentally-determined design parameters.

The available NPSH (net positive suction head) for the SNAP I pump was found to be approximately 0.30 feet of mercury. With only this small NPSH available to the pumping system the velocity head in the pump inlet must be maintained at a low value. In theSNAP I system, 40% of the available head was converted into velocity. With the use of a jet pump ahead of the impeller, and retaining the same velocity, it was felt that the jet pump would overcome all the additional losses, such as friction in the pump inlet line from the subcooler to the pump inlet, and the dynamic depression on the pump inlet blades. In order to have minimum entrance losses, there should be a negligible change of velocity from the pump inlet line to the impeller inlet where energy is added to the fluid. Using these assumptions the inlet to the pump was designed.

Front face leakage or recirculation is considered as a function of ideal head. This leakage was calculated by extrapolating the performance vs front face clearance data to zero front face clearance. Thus, the total flow lost to recirculation and leakage and the lost power required to supply this leakage may be calculated.

If cavitating conditions exist in the pump inlet, the hydraulic efficiency of the impeller is lower than normal design procedure would dictate. To compensate for this lower hydraulic efficiency, a larger diameter impeller is necessary. The determination of the magnitude of this lower hydraulic efficiency can only come from test data. The test data from the tests of the shaft pumps may be used as reasonable estimates for the vaned pumps. Once the hydraulic efficiency of two pumps is assumed equal, the pump affinity laws can be used to make any necessary changes. The best performance of the shaft pumps indicated an expected hydraulic efficiency of $\approx$66%. The outside diameter of the impeller was calculated to be 0.40 inches which provided an impeller tip velocity of 70 fps.

The pump performance mya be appreciably affected if erosion, corrosion, or contamination deposits may be considerable when compared to the size of the discharge flow passage from the pump. Therefore, the pump must have clean, deaerated mercury.

Since the calculated inlet blade angle is very shallow, the number of blades is limited by the size of cutters available. The blade thickness at the impeller eye is assumed negligible, since very sharp edges are desired. Using actual pump geometry and assuming prerotation of the fluid, the required NPSH is 1.6 ft or 9.0 psi. Since the NPSH required is greater than that available, a jet pump was used to increase the inlet pressure to the impeller.

5.1.2 Jet Pump

In this application the successful operation of the jet pump is required in order for the centrifugal pump to meet its design requirement since the jet driving power comes directly from the centrifugal pump discharge. An optimization was made to determine the amount of centrifugal pump flow to be recirculated to drive the jet. This optimization is based on:

1. Centrifugal pump output

2. NPSH required by the impeller

3. Developed pressure of the jet pump

4. Cavitation limit on the jet pump

Caviation must be considered in the throat of the jet pump since all of the pumped fluid must pass through a restricted area before it is given additional energy by the high velocity jet. The weighing of these parameters indicated that approximately 13% of the impeller discharge flow should be recirculated.

The design configuration and performance of the jet pump was based on a combination of Stepanoff's empirical curves, the impulse and momentum equations, and experimentally determined jet pump test results. The assumed nozzle discharge coefficients and mixing efficiencies were based on results obtained from SNAP I Jet Pump Development testing.

### 5.1.3 Volute Design

The volute design was based on the empirical method of Stepanoff which amounts to designing an efficient collector to take the fluid from the impeller and deliver it to the pump discharge line. The main parameter which must be established is the average volute velocity, $c_3$. Stepanoff has determined an experimental relationship for $c_3$ as follows:

$$c_3 = K_3 \sqrt{2gH}$$

where $K_3$ is a function of specific speed.

The accepted practice for present centrifugal pumps is to design for a constant average velocity ($c_3$) for all sections of the volute which means that volute areas are proportional to their angular advancement from the cut-water. The total pump capacity must pass through the throat section and any other section has only partial capacity. The throat area can be found by the following expression:

$$A_t = \frac{Q}{C_3} = 1.34 \times 10^{-3} \text{ in}^2$$

In order to have continuity of volute elements the volute shape must fit the following equation:

$$A_5 = b_3 D_3 \pi \sin \alpha_v$$

where $\alpha_v$ is the volute angle and also the angle at which the fluid enters the volute. To simplify fabrication and to provide minimum deviation from the average volute velocity, a rectangular section expanding radially in an Archimedes spiral was used.

Once the fluid is collected in the volute, it is taken off in a straight diffusing section. The only velocity which can be converted into pressure in this diffuser is the volute velocity $c_3$.

### 5.1.4 Cavitation

Since cavitation presents a severe design problem for the SNAP I pump design, it should be discussed separately for the following reasons:

1. The exact prediction of unworkable cavitating conditions is doubtful

2. Cavitation is a limit on a design, not an absolute design factor

3. The overall pumping requirements must be optimized against the cavitation limits to obtain a suitable pump.

Cavitation is difficult to predict since it occurs at any place in the system where the pressure of the liquid reaches the vapor pressure of the liquid at the corresponding temperature. These low pressures can be caused by turbulence, vortex motion of the fluid, rapid changes in velocity of the fluid either in direction or magnitude, or hot spots in the system. Therefore, to reduce the probability of cavitation occurring, all flow passages must be smooth with no sharp turns or sudden changes in area. In addition, the inlet blade loading of the impeller should be gradual to reduce the pressure drop (dynamic depression)caused by changing the fluid velocity.

Two factors which must be known to determine the cavitation limit of a pump are the net positive suction head available ($NPSH_a$) and the net positive suction head required ($NPSH_r$). The determination of the $NPSH_a$ is relatively simple, but the $NPSH_r$ is difficult to determine. There is one method available for predicting the start of cavitation for low specific speed pumps based on the inlet velocities of the pump and an experimental coefficient $\lambda$. Since pressure is converted into velocity to obtain flow and centrifugal force, this velocity can be used to estimate incipient cavitation, and, in turn, give the NPSH required to overcome cavitation. The empirical expression for this relationship is:

$$NPSH_r = \frac{C_1^{\,2}}{2g} + \frac{\lambda W_1^{\,2}}{2g}$$

where $C_1$ = average absolute fluid velocity through the impeller eye.

$W_1$ = average relative fluid velocity at the impeller entrance

$\lambda$ = an experimental coefficient

This equation was used to determine the impeller requirements after the inlet velocity $C_1$ was established. Test data indicated reasonable experimental correlation with the equation. This equation was used to determine the optimum diameter $D_1$ to provide the minimum $NPSH_r$ by rearranging and differentiating the equation and solving for a minimum value of $NPSH_r$. The resulting equation is

$$D_{1\,min} = (1 + \lambda)^{1/6} \left( \frac{2 K_c}{K_u} \right)^{1/3}$$

$$\text{where} \quad K_c = \text{flow parameter} = \frac{4Q}{\pi \rho \, 60}$$

$$\text{and} \quad K_u = \frac{N \pi}{60}$$

This calculated minimum inlet diameter was applied to the impeller designs as an average inlet blade diameter.

A plot of this equation indicates the importance of using the correct diameter to obtain the minimum $HPSH_r$ since the $NPSH_r$ requirements rise rapidly on either side of the minimum value.

5.1.5 System Integration

Although the pump output performance is an extremely important characteristic, there are three secondary characteristics which must be determined and evaluated in order to ascertain the effect of the pump on the system. These are:

1. Power needed to drive the pump
2. Thrusts resulting from the pump
3. Fabrication and assembly of pump parts

5.1.5.1 Pump Power Requirements

The pump power requirement was estimated by an analysis of the hydraulic, volumetric, and mechanical losses associated with pumping. The summation of these losses, added to the pump hydraulic output as established by the system requirements, gives the power needed to drive the pump.

5.1.5.2 Pump Thrust

The axial thrust in a centrifugal pump is a function of pressure and area. The pressures and areas involved include the inlet area, total impeller area, shaft area, inlet pressure and discharge pressure. The addition of back vanes on the impeller or a leakage path along the shaft alters the pressure distributions and thus makes accurate computation of the axial thrust difficult. The thrust is more accurately determined from test data.

5.1.5.3 Fabrication and Assembly

Fabrication of the impeller and volute imposes a difficult machining problem due to the size of these parts. The distance between adjacent impeller blades must be laid out carefully in order to allow room for a cutter. Since the minimum practical cutter size is approximately 0.030 inch diameter, there is not only a limit on blade spacing, but blade thickness must also be controlled carefully. In order to keep good impeller proportions, the blade thickness may be tapered from the O.D. to the I.D. A plain blade (constant radius curve) is the only type that could be machined, since machining tolerances would not allow a mixed flow blade.

Inspection of these small parts also presents a problem. After trying several methods without success, the impeller and volute curves were placed upon a grid system and measurement taken from a fixed reference point.

The attachment of the impeller to the extended shaft was a difficult problem due to its extremely small size. As the final solution, the impeller was threaded on the extended shaft and pinned.

### 5.2 Jet-Centrifugal Pump Performance

Basic pump performance was obtained on the pump component test rig at design and off-design conditions. Figure 4-8 shows the jet-centrifugal pump test assembly with the jet pump housing.

Evaluation of the performance of the basic four-vaned impeller stage is included in section 4.3. The development testing included the following investigations:

1. Effect of vane configuration (Figure 4-5)
2. Performance vs Speed (Figure 4-6)
3. Head, Power, and Efficiency at design speed and inlet pressure (Figure 4-9)

The general performance of the four-vaned radial impeller with the jet boost stage is discussed in section 4.5. Specific characteristics of the jet-centrifugal pump will now be discussed.

#### 5.2.1 Pump Design Performance and Effect of Jet Pump

Figure 4-9 shows the overall jet-centrifugal pump characteristics at approximately .003 inch front face clearance (head, power, and efficiency at design speed and inlet pressure). Since this curve shows the operation of the four-vaned impeller with and without the jet pump, the overall improvement provided by the jet pump is clearly indicated. The four-vaned impeller had a maximum capacity of approximately 10 lb/min at 300 psi while the same impeller with the jet pump boost operated stably at approximately 15 lb/min and 400 psi. This high level of performance is due to the fact that the addition of the jet boost stage eliminated the detrimental effect of cavitation on pump performance. With the increased NPSH available for the impeller stage, the concept of an oversized impeller diameter to meet the specified capacity was revised.

At design conditions of 40,000 rpm and 1.9 psia inlet pressure, the pump input power was approximately 70 watts and the overall pump efficiency was 27%. Excellent suction capabilities were indicated by satisfactory pump operation at the overall design suction specific speed of 40,000 rpm, which was possible due to the jet boost.

5.2.2 Pump Performance Map

A SNAP I pump performance map of Pump Discharge Pressure vs Diffuser Flow at various speeds and front face clearances is plotted in Figure 5-1. This jet-impeller performance map was obtained from the best available data of the pump-bearing and pump component tests at design inlet pressure with room temperature mercury. Actual data points are plotted on the figure.

5.2.3 Cavitation Characteristics

Figure 5-2 illustrates the cavitation characteristics of the jet centrifugal pump at 40,000 rpm with room temperature mercury from Pump-Bearing Tests. Incipient cavitation was observed at a NPSH of approximately 2.5 psi, but stable operation was maintained to 1.3 psi. No significant decrease in performance was noted while decreasing the inlet pressures at lower speeds and flows. Some slight cavitation damage was noted near the inlet tip of the impeller and may have been incurred during over-capactiy testing.

5.2.4 Effect on Inlet Temperature on Pump Performance

An evaluation of the effect of temperature on pump performance was obtained in the pump component test rig in the early phase of development. Figure 5-3 shows the test results of the four-vaned impeller in the jet housing with an interim design jet pump for 75$^{\circ}$ and 330$^{\circ}$F mercury inlet temperatures. The pump performance decreased slightly with the increased inlet temperature at 40,000 rpm and 2.0 psia inlet pressure. As the development progressed, the full pump discharge pressure was used to drive the jet pump and a higher level of overall pump performance was obtained.

5.2.5 Jet Pump Performance

The general operating performance of the jet centrifugal pump was satisfactory. Head and flow requirements were met at the design inlet temperature and pressure. Very few signs of wear or damage were observed on the pump component test rig.

Due to the low pressures in the pump inlet, it was inadvisable to put a pressure probe after the jet pump. Instead of disturbing the stream with such a probe, the increase in centrifugal pump performance was used to indicate jet pump output. The final jet pump gave the centrifugal pump impeller an increase in performance at the b.e.p. equal to an inlet pressure of approximately 9 psia without the jet. It was then assumed that the jet pump was raising the incoming mercury from 1.9 psia to 9 psia, which indicates an efficiency of the jet pump of approximately 14%.

PUMP DISCHARGE PRESSURE VERSUS DIFFUSER FLOW
PUMP INLET PRESSURE = 1.9 PSIA
PUMP INLET TEMPERATURE = 75°F

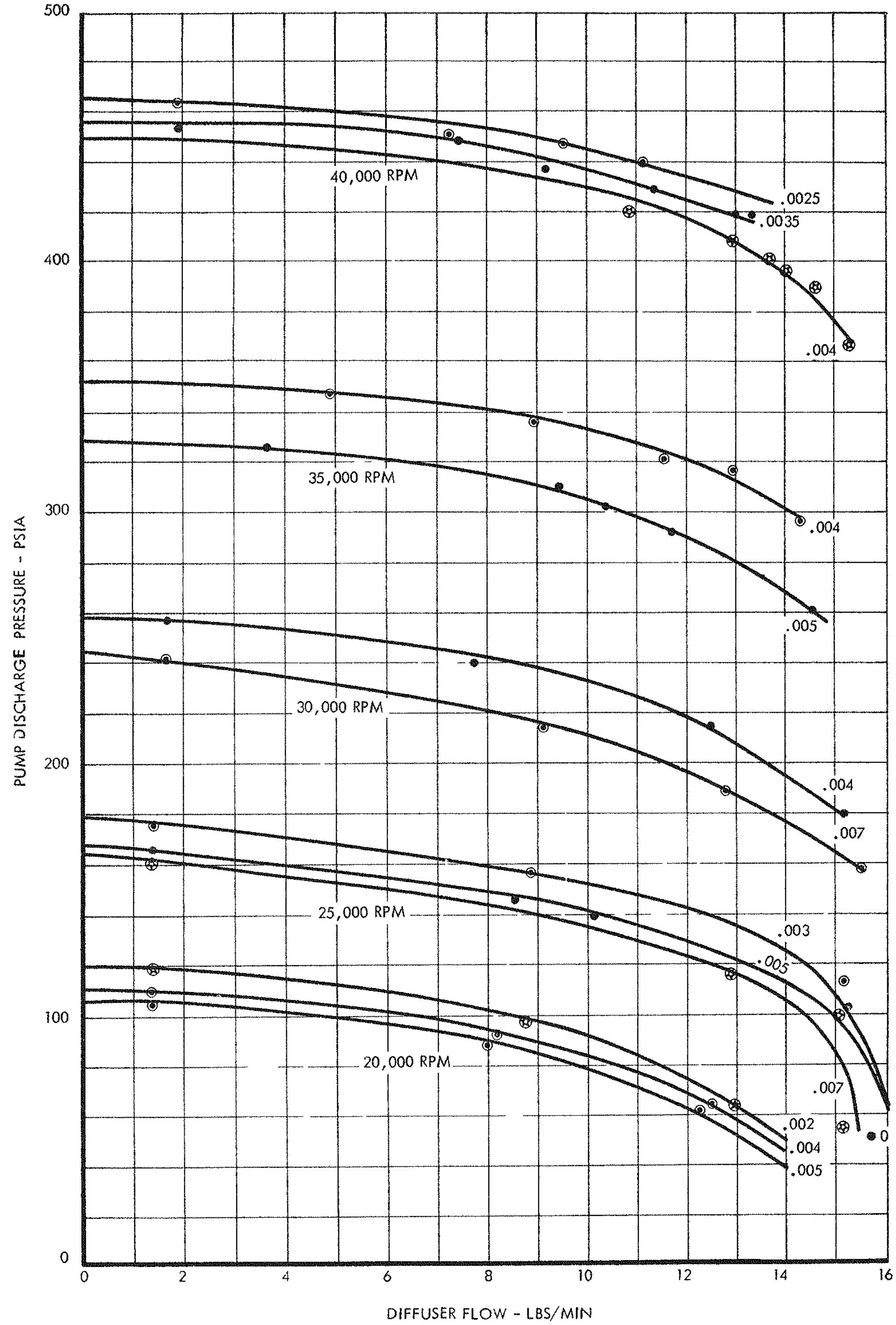


FIGURE 5-1

JET CENTRIFUGAL PUMP CAVITATION CHARACTERISTICS

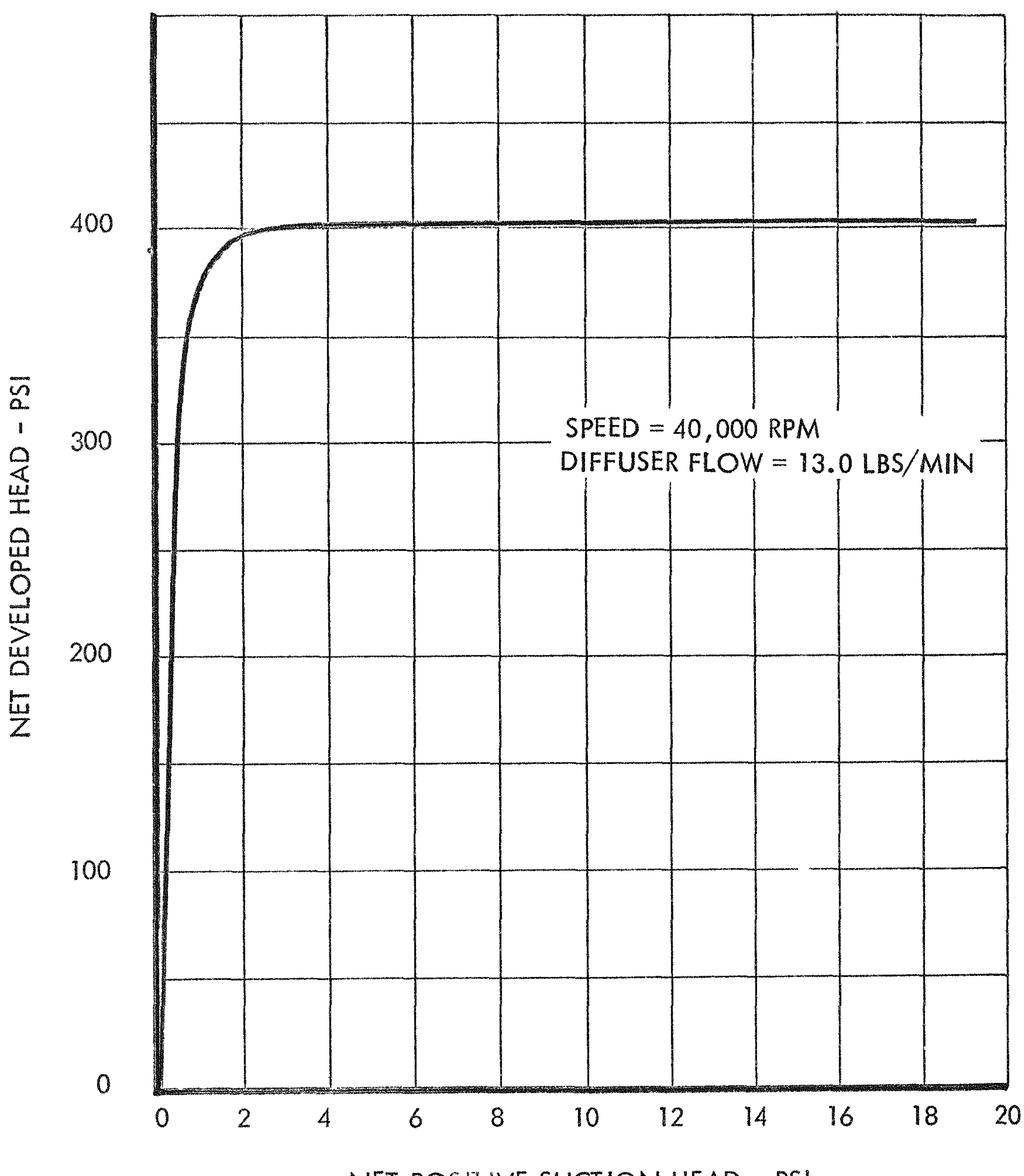


FIGURE 5-2

EFFECT OF INLET TEMPERATURE ON PUMP PERFORMANCE

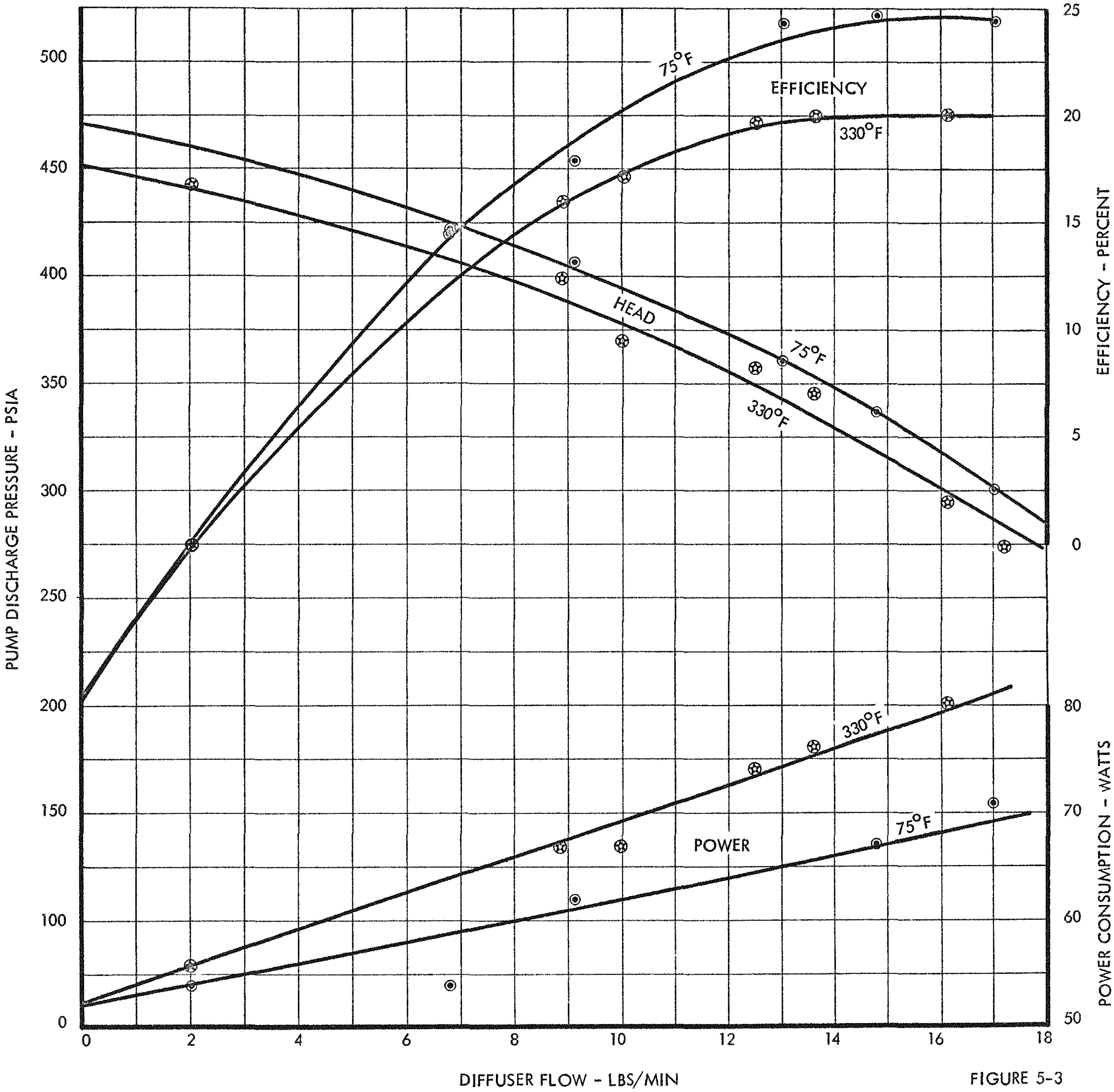


FIGURE 5-3

### 5.2.7 Pump Power and Thrust

The measured pump input power of approximately 70 watts at design conditions was obtained on the pump component test rig. The pump input power as measured by the calibration of the electric drive motor was correlated by the cradled dynamometer results.

Pump thrust was measured by the pump drive motor dynamometer in the pump component test rig and by the hydrosphere bearing thrust parameters in the pump-bearing subsystem tests. Pump thrust at design capacity was measured to be 17.5 lb acting on the back face of the impeller which is typical of single stage open impellers.

### 5.3 Pump-Bearing Subsystem Performance

A cross-section of the SNAP I jet centrifugal pump-hydrosphere bearing combination test fixture is shown in Figure 5-4. It is essentially a dual hydrosphere bearing assembly consisting of a shaft incorporating two hydrosphere bearings and a small diameter shaft extension with an end mounted radial pump impeller supplemented by the jet boost stage. The integral rotating shaft is supported in two hemispherical bearing sockets. Power for the unit is provided by an air turbine mounted between the bearings. The pump-bearing configuration represents conditions of operation which are unconventional to normal centrifugal pump operation and which require special testing and analysis. Testing was conducted to investigate the following areas:

1. Effects of pump front face clearance - the pump impeller clearance is determined by the bearing performance which is a function of the preset total axial clearance and thrust loading.

2. Pump axial thrust - the pump thrust combined with turbine and alternator thrust loads determines the axial location of the shaft and, as mentioned above, affects pump performance.

3. Pump leakage - leakage from the bearing supply through the close clearance annular flow restriction is into the pump cavity and affects the performance as added flow component in the volute and as hydraulic loss from the recirculating leakage.

4. Priming - pump priming and low pressure operation require investigation.

5. Pump operation in the system.

The Free Running Bearing Test Rig (Air Turbine Drive) was modified to incorporate provisions to test a pump-bearing combination. This test rig was used for the final evaluation of the SNAP I pump before incorporation into the prototype package. In the test arrangement, axial thrust applied to the bearings was varied externally in order to change pump front face clearance. Also, the annular flow restriction and leakage conditions of the final package were simulated.

## PUMP-BEARING COMBINATION TEST FIXTURE

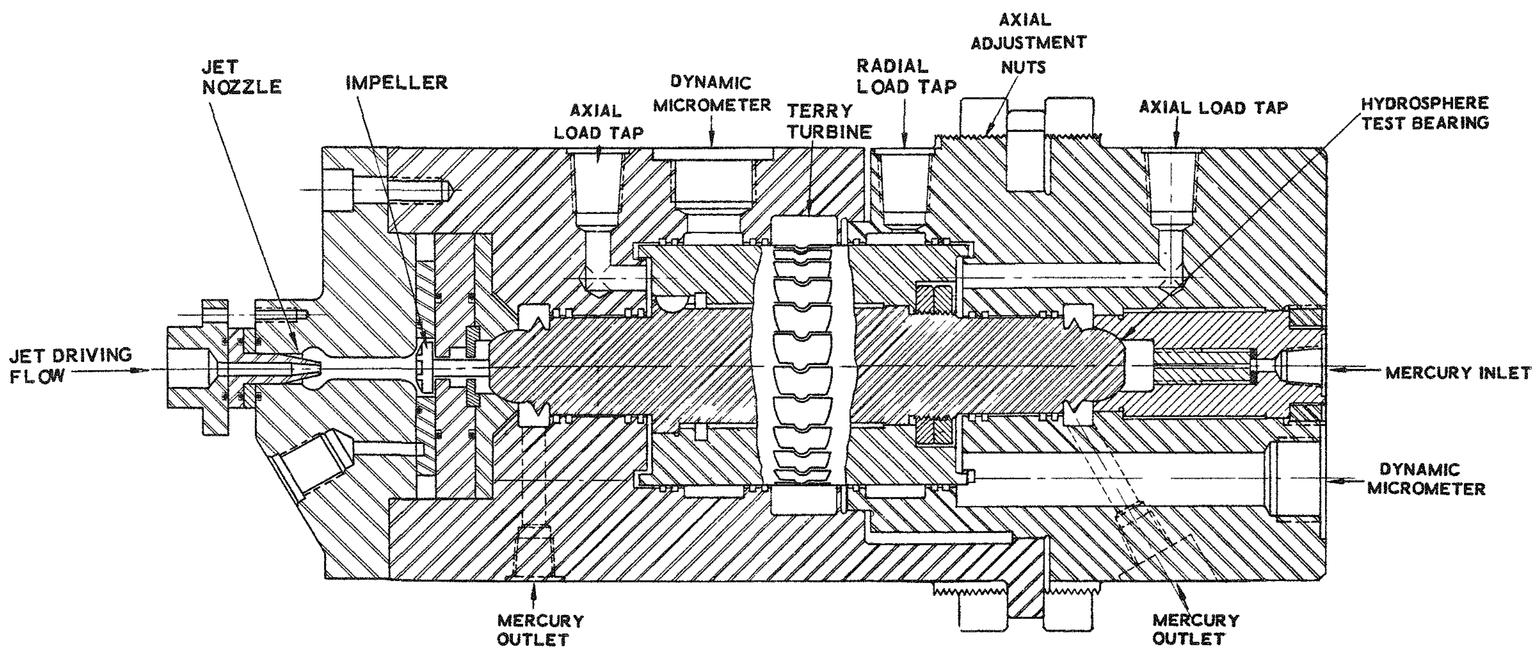


FIGURE 5-4

A photograph of the hydrosphere bearing shaft with the overhung centrifugal pump impeller is shown in Figure 5-5.

5.3.1 Combined Pump-Bearing Operation

The jet-centrifugal pump hydrosphere bearing combination operated satisfactorily both in separate circuits and when hydraulically coupled together up to 45,000 rpm. Combined pump and bearing performance was obtained with the pump supplying mercury to the bearings. The SNAP I system was being simulated hydraulically with the bearing supply valve wide open and the bearings taking full pump discharge pressure. Also, approximately 2.6 lb/min was being pumped through the by-pass line to simulate boiler flow. Axial thrust loads were then applied to the rotor in both directions. Applying thrust loads to increase the pump front face clearance caused the pump head and flow to drop off. When loading the pump end bearing, the discharge pressure increased due to the decreased pump front face clearance.

5.3.2 Pump Performance

Figure 5-1 shows pump performance at 40,000 rpm over the entire range of capacity. The head versus flow curve was obtained with the pump operating in its own hydraulic circuit and the curve is plotted to show the actual flow through the pump including the recirculating leakage and jet flows. The useful flow is the flow available for the boiler and the bearings and may be calculated by subtracting the recirculating leakage and jet flows from the total flow. The general performance of the pump is approximately the same as that observed in the pump test rig data at inlet pressures above design and at large clearances.

A SNAP I System - Pump Performance Map is included in Figure 5-6. Superimposed on the pump performance map are the estimates of the various flow requirements of the system, such as jet flow, boiler flow, leakage flow, and bearing flow. At the system design pressure of 287 psia the flow requirements of the system were established as follows:

| | |
|---|---|
| Jet Flow | 1.5 lb/min |
| Boiler Flow | 2.0 lb/min |
| Leakage Flow | 0.8 lb/min |
| Bearing Flow | 6.0 to 10 lb/min |

The estimated variation of these flows at different pressures was calculated and plotted on the curve. Since an auxiliary pump supplied system flow requirements during startup, the system pump operated at shut-off against a check valve until it developed a pressure greater than the auxiliary pump. After the speed of the turbo-machinery package increased to allow the system pump to supply the system, the auxiliary pump was shut down.

The system operating lines are indicated for various bearing flows on the upper right hand portion of Figure 5-6. For a fixed system any change in speed of the turbo-machinery

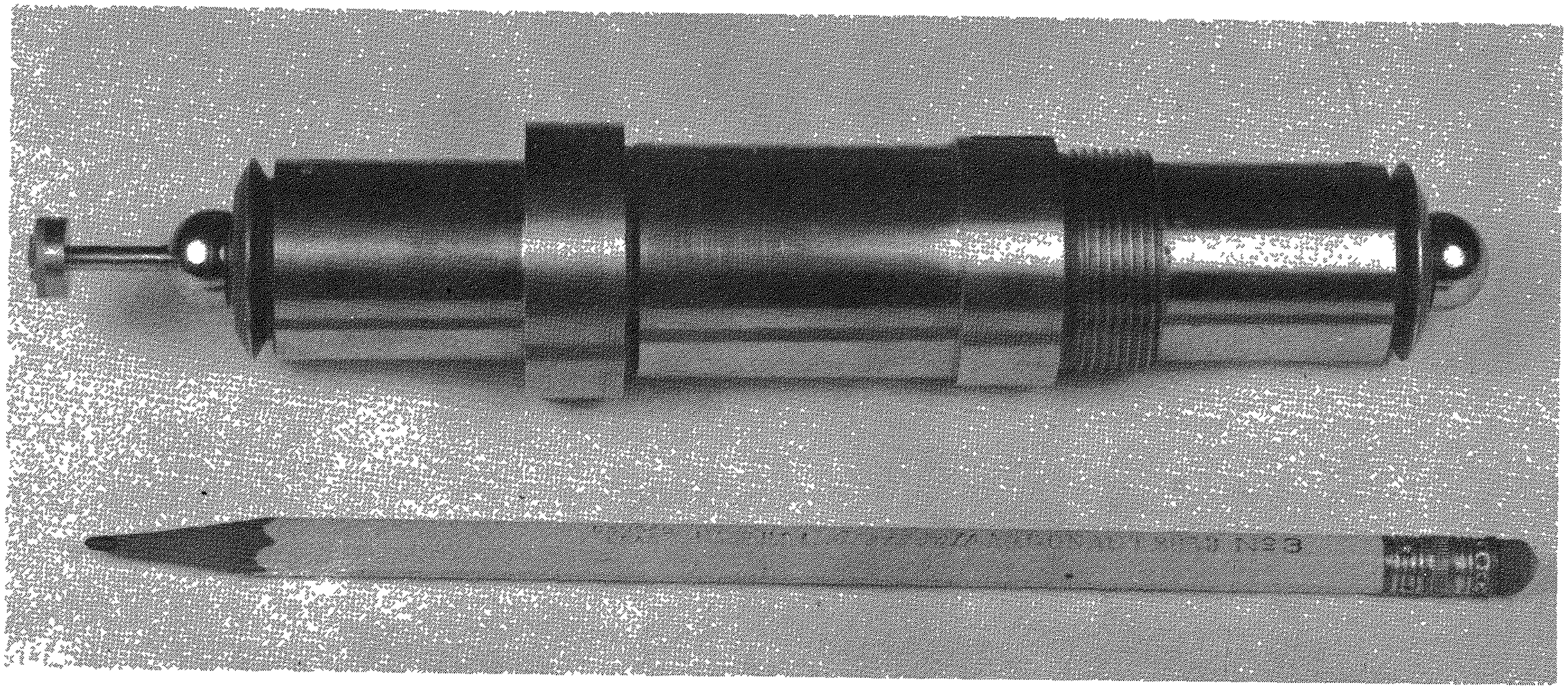

SHAFT FROM PUMP-BEARING COMPONENT TEST

FIGURE 5-5

PUMP PERFORMANCE MAP
PUMP DISCHARGE PRESSURE VERSUS DIFFUSER FLOW
AT VARIOUS SPEEDS AND FRONT FACE CLEARANCES

PUMP INLET PRESSURE = 1.9 PSIA
PUMP INLET TEMPERATURE = 7.5°F

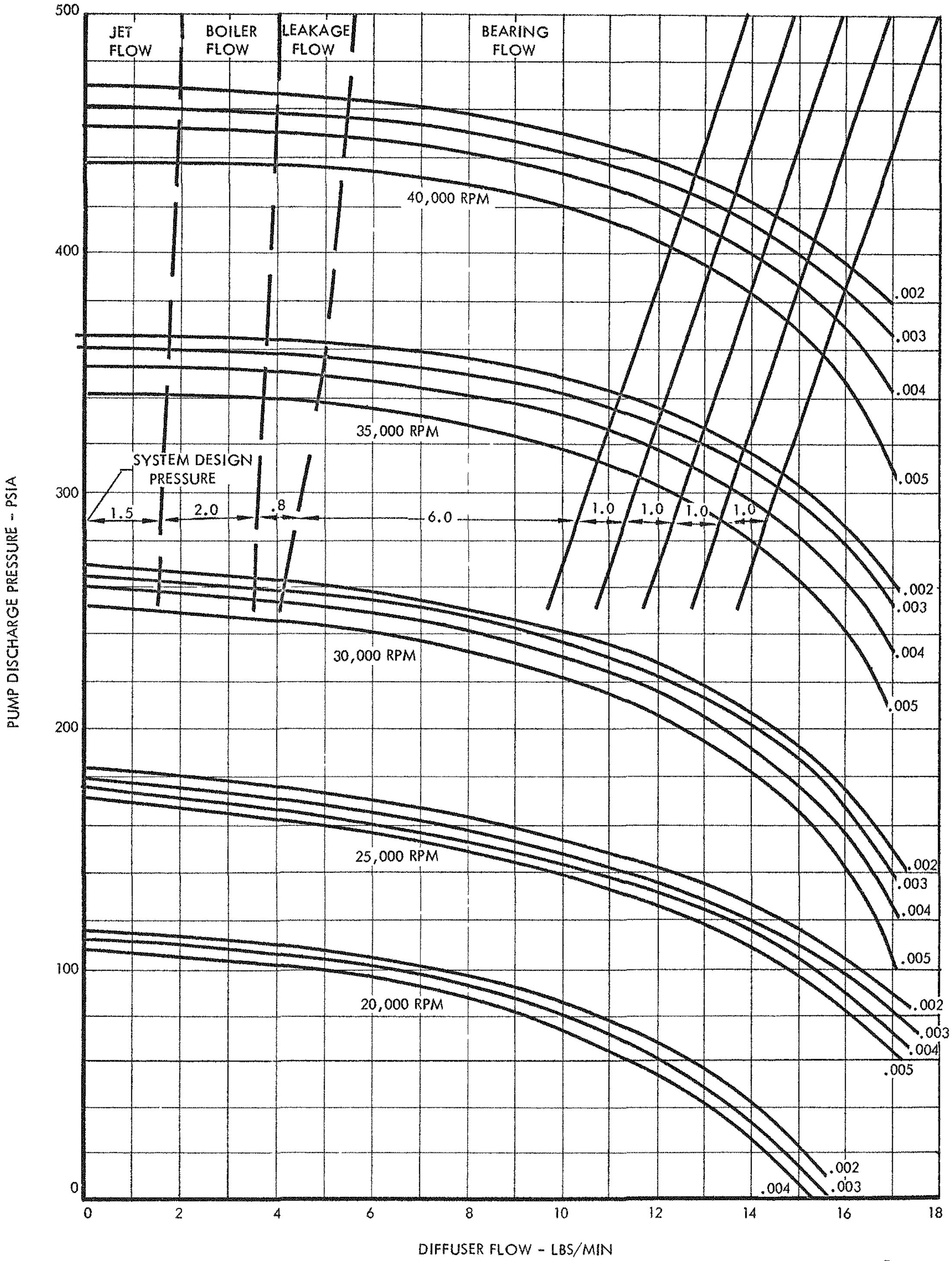


FIGURE 5-6

package changes the pump discharge pressure and the system follows the appropriate system operating line. Thus the approximate pump and system operating conditions can be predicted if the pump speed, front face clearance, and total system flow are known.

### 5.4 Pump Performance in System Tests

The first SNAP I turbo-machinery package was the Turbine-Alternator Test Package (TATP) used to evaluate turbine performance. The TATP package consisting of a three stage mercury vapor turbine and a loading alternator supported on mercury lubricated bearings was modified to incorporate the mercury pump. The resulting package was designated the Turbine-Alternator-Pump Package (TAPP). Testing of the TAPP unit in the Mercury Vapor Breadboard Test Facility established the operational ability of the pump in its final application.

The first prototype SNAP I turbo-machinery package - the Prototype Test Package (PTP) - was designed to incorporate the develped components, including the overhung jet-centrifugal mercury pump, the mercury lubricated hydrosphere bearings, a three-stage axial flow turbine, and a radial gap alternator. Preliminary testing of the PTP package was accomplished in the Mercury Vapor Breadboard to establish operational ability and performance. Later system tests were conducted in the Systems Test Enclosure (STE) of the complete SNAP I Power Conversion System, including the PTP turbo-machinery package, boiler, condenser, and auxiliary equipment.

#### 5.4.1 Turbine-Alternator-Pump Package Tests (TAPP)

The pump objective of the TAPP tests was to evaluate overall pump performance with the pump operating in its own circuit and then attempt a coupling of the pump output to the bearing supply to eliminate the auxiliary supply pump from the system.

System test difficulties prevented the acquisition of the desired steady-state pump data, but pump performance was found to be satisfactory. More notable, however, the pump flow was coupled to supply the bearings, with complete success; performance was stable and no adverse interactions were present.

#### 5.4.2 Prototype Test Package Tests (PTP)

Experimental testing of the PTP package had the following pump objectives:

1. To establish operational ability of the SNAP I pump and bearings while coupled.

2. To obtain pump performance at design conditions to compare with design specifications.

3. To obtain pump performance at various speeds to compare with the pump performance map obtained from the pump-bearing subsystem tests.

4. To determine endurance capability of the hydrosphere bearings and the jet-centrifugal pump.

The pump and bearings operated satisfactorily at design speed and pump inlet pressure while the package ran on hot mercury vapor for 48 hours continuous running. The total dynamic time accumulated on PTP I while running on both nitrogen and mercury vapor at varying spees and pump inlet pressures was $\approx$67 hours.

Predicted pump performance was obtained during the early PTP tests but these performance levels were not completely reproduced in later operation due to the presence of non-condensibles, thermal expansions, or contamination of the pump flow passages. The high level of pump performance is obtained with a clean, deaerated supply of mercury. Although the pump performance was lower than predicted during some of these tests, the pump output was stable and sufficient to allow the pump to supply the bearings while running at design conditions with no apparaent decay in performance with time.

## 6.0 PUMP TEST FACILITIES

The preliminary testing of the mercury pump was accomplished in the Feasibility Bearing Test Rig. The major pump development work was conducted on the Pump Component Test Rig, which was designed, fabricated, and built under this project. Final SNAP I pump testing included tests of the Pump-Bearing Combination Test Package in the Free Running Bearing Test Rig, and tests of the system test packages in the System Test Rigs.

### 6.1 Feasibility Bearing Test Rig (Preliminary Pump Testing)

The preliminary testing of the mercury pump was accomplished by incorporating the test pump model on the initial Feasibility Bearing Test Rig.

Figure 6-1 indicates the pump housing shown on the bearing test rig. Several configurations of pump shafts were tested with this first housing. The bearing test rig allowed the pump to rotate at 40,000 rpm and the measurement of the pump torque. The mercury supply heaters on the bearing test rig heated the mercury to temperatures as high as 500°F. By controlling the reservoir level the pump inlet pressure was varied to simulate conditions of the final power conversion unit. The leakage and pump outlet flow were measured by collecting the flow. Alignment of the pump shaft and housing was critical due to the close tolerances required in the pump to prevent excessive leakage.

### 6.2 Pump Component Test Rig (Development Pump Testing)

Test facilities progressed with pump development as test requirements changed and became more complex. The basic pump component test rig is shown schematically in Figure 6-2. A photograph of the Pump Component Test Rig is included as Figure 6-3. A brief description of test rig components follows.

#### 6.2.1 Drive and Power Measurement

A precision built motor with an integrated rigid spindle in which the pump shaft was held by a collet chucking device was selected as a drive. Motor speed was regulated by a rheostat control and was indicated by frequency signals from a magnetic pickup at the chuck.

Power measurements were obtained by electrical calibration of the drive motor using a friction brake. Results were plotted on an electrical input vs brake power output calibration curve.

A transmission dynamometer was also designed and built in which the drive motor was cradled and the reaction torque was measured by a double orifice flapper pneumatic transducer. A pneumatic pickup was also incorporated which would measure pump axial thrust. Figure 6-4 shows the general arrangement of the cradled dynamometer.

#### 6.2.2 Flow Measurement

Two methods of flow measurement were investigated. Magnetic flow meters proved to be

PUMP TEST ON BEARING TEST RIG

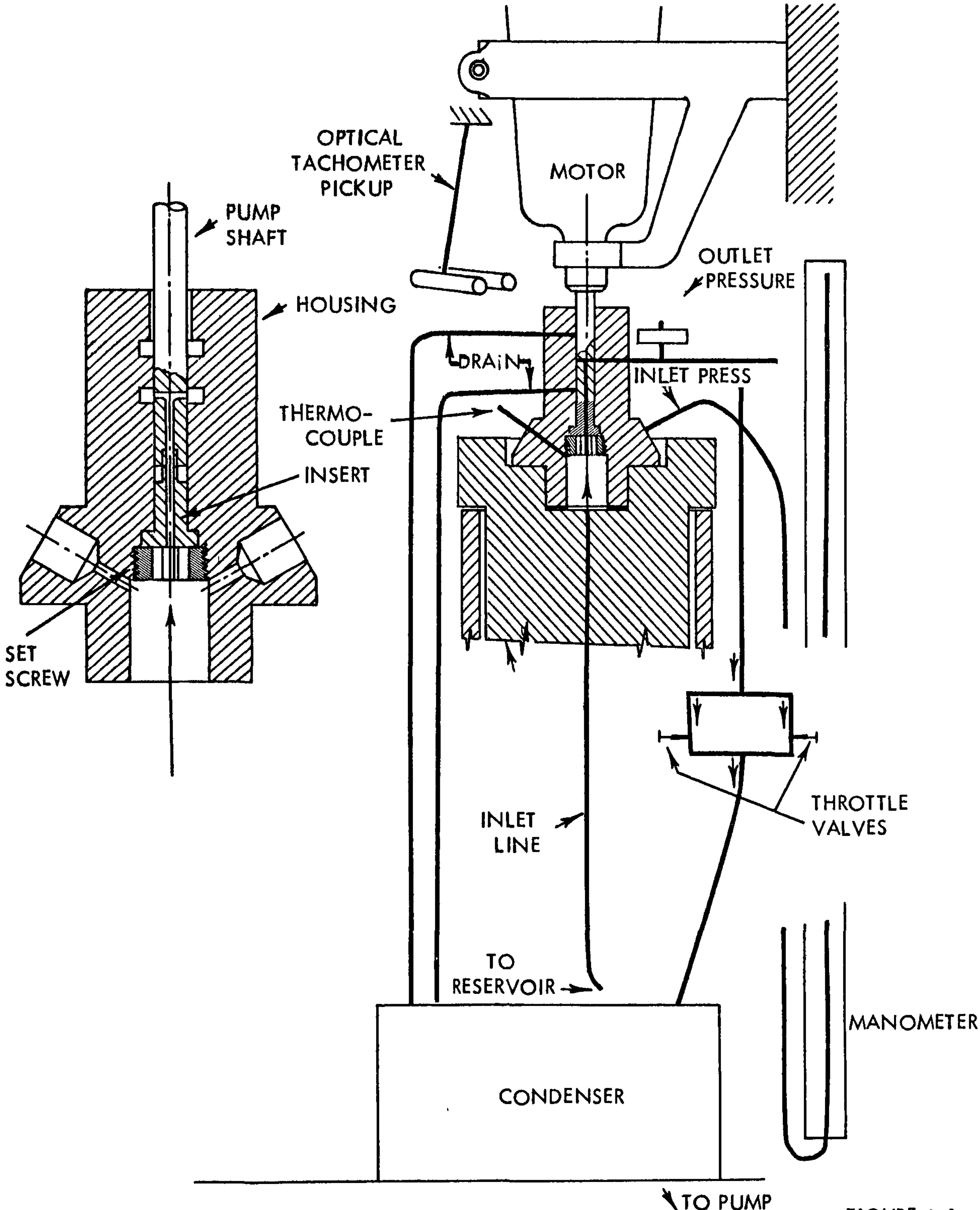


FIGURE 6-1

PUMP TEST RIG FLOW SCHEMATIC

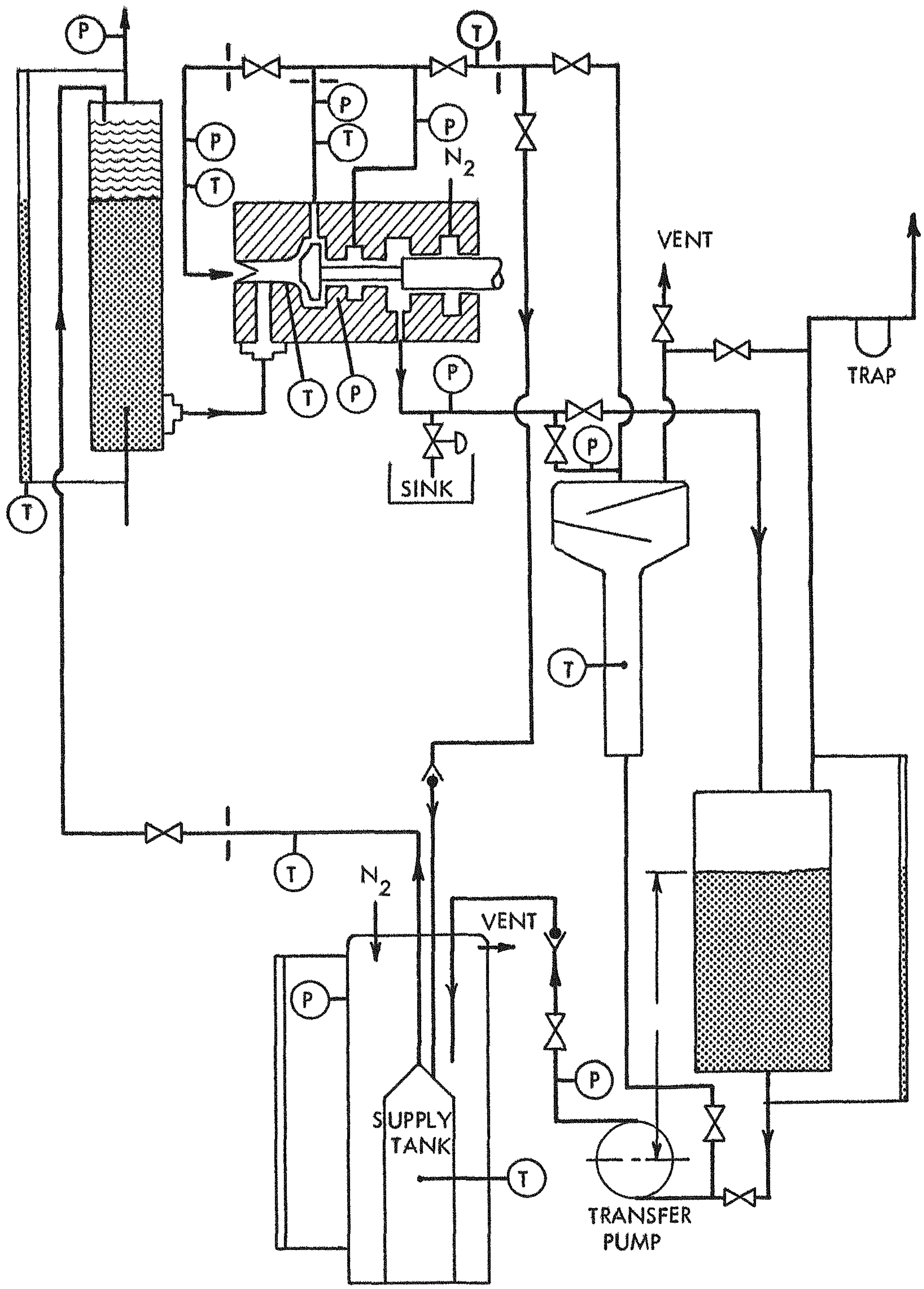


FIGURE 6-2

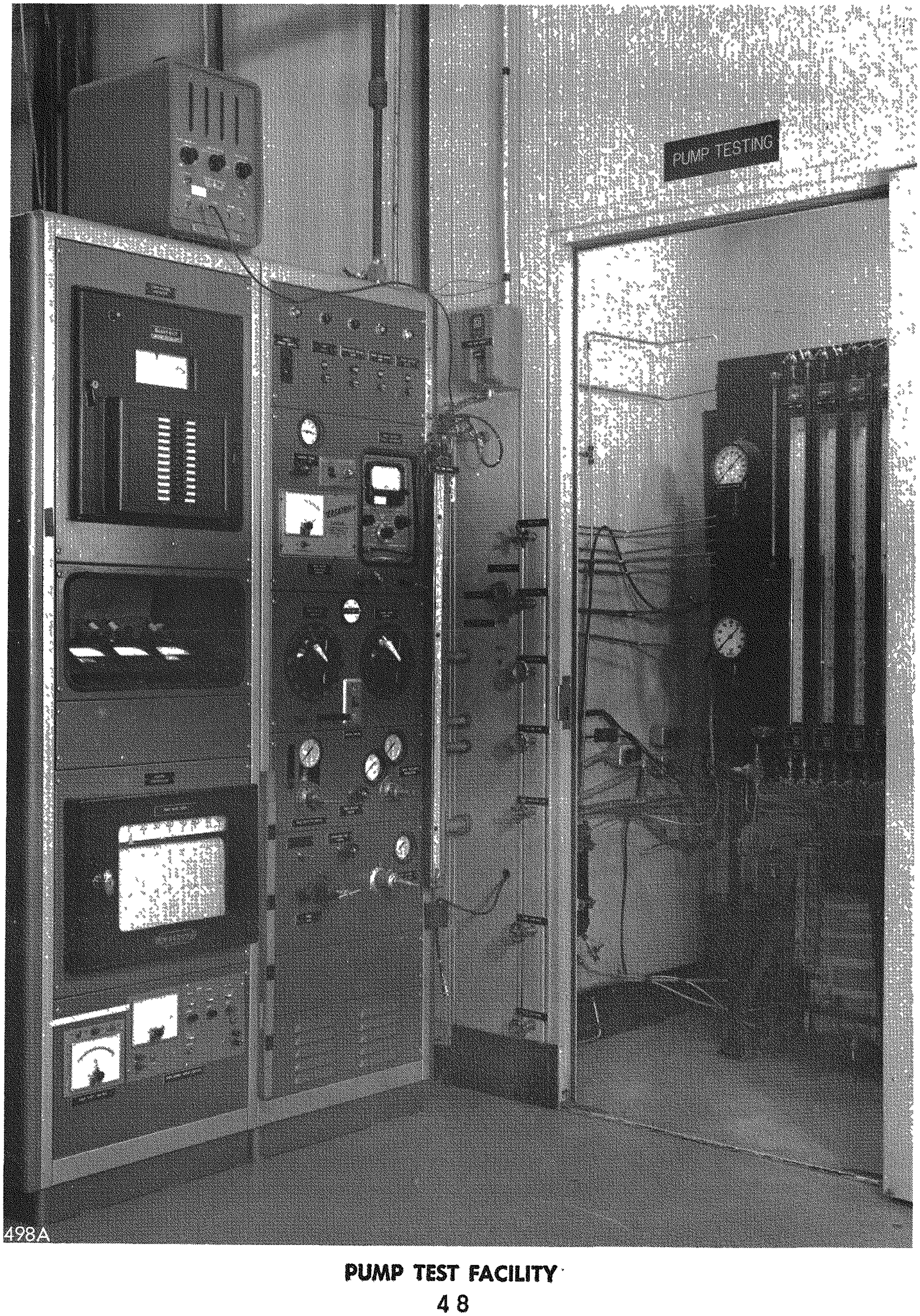


**PUMP TEST FACILITY**



FIGURE 6-3

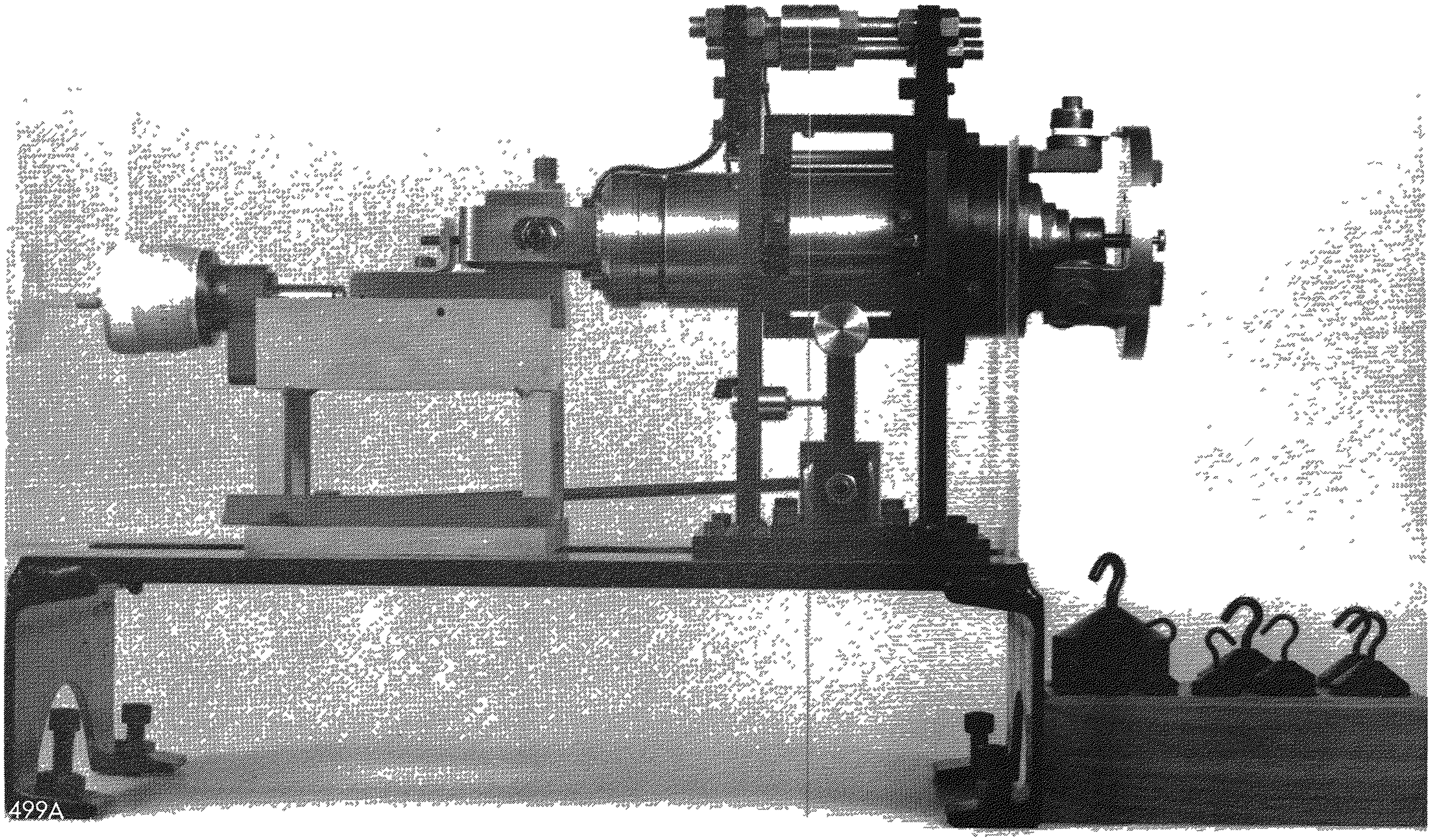


PUMP DYNAMOMETER

FIGURE 6-4

unsatisfactory because of electrode wetting and deterioration problems. They were replaced by sharp-edged orifice plates and 30" inverted U-tube manometers. The orifices were calibrated by weight flow checks and were found to yield accurate flow measurement.

### 6.2.3 Pressure Measurement

High pressure measurement was obtained with stainless steel bourdon tube gages. U-tube manometers were used for low and vacuum pressure measurements.

### 6.2.4 Temperature Measurement

Temperature measurements utilized iron-constantan thermocouples in conjunction with a twenty-four switch station Brown temperature recorder and a single channel $0^{\circ}$ - $800^{\circ}F$ automatic Weston strip chart recorder.

### 6.2.5 High Temperature Operation

High temperature operation was obtained by preheating the fluid mercury with electrical resistance heater coils which were submerged in the supply reservoir. Temperature control was accomplished by an indicating controlling pyrometer.

### 6.2.6 Pump Inlet Conditions

Accurate control of the pump inlet conditions was obtained through the use of a specially designed inlet separator tank. The liquid mercury was admitted at the top of the vessel and passed by gravity through a series of baffled trays. Full or partial vacuum was drawn on the vessel by a vacuum pump. The liquid level in the tank was observed through a sight gage and the height above pump centerline was controlled by inlet flow. This method not only accurately controlled the pump inlet pressure, but also insured that the mercury was degasified. An added feature of this system was that it simulated an actual subcooler plus pump inlet line for ground operation (gravity field).

## 6.3 Pump-Bearing Subsystem Test Rig

The Free Running Bearing Test Fixture was modified to incorporate provisions to test a pump-bearing combination as shown in Figure 5-4.

The rig incorporated flexibility to permit dual bearing (hydrospheres, or journals and thrust bearing) operation and evaluation of the pump-bearing combination performance in a simulated package. The drive to rotate the pump and bearings was a Terry-type turbine supplied with 100 psi air. An air preheater was available to heat the turbine air. Incorporated in the test fixture were pressurized air load pads which could apply axial and radial loads simultaneously or individually to the bearings.

The bearing lubricant was supplied from a pressurized reservoir with $N_2$ cover gas or the System jet-centrifugal pump. A Lapp Pulsafeeder proportioning pump which delivered up to 40 lb/min of liquid mercury at 300 psig supplied the reservoir. Facilities were incorporated into the test rig to enable the bearing supply, bearing socket, and pump discharge and back face pressures to be recorded with pressure transducers and a 6 channel osciliograph. Figure 6-5 is a photograph showing an external view of the Free Running Bearing Test Rig and instrumentation.

Figure 6-6 shows the pump-bearing combination test fixture installed in the FRR test rig. The system pump is on the left end of the test fixture with the pump inlet separator slightly to the left of the pump.

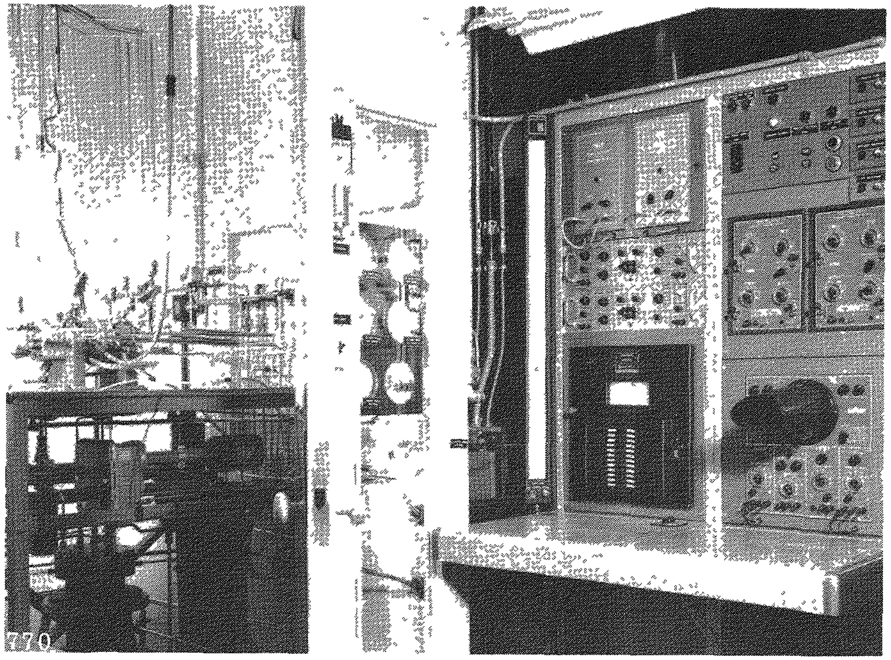

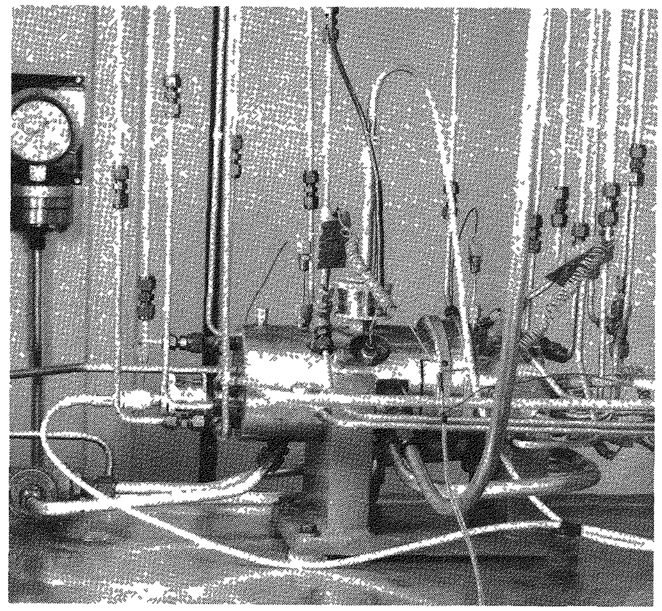

FREE RUNNING MERCURY BEARING TEST RIG

FIGURE 6-5

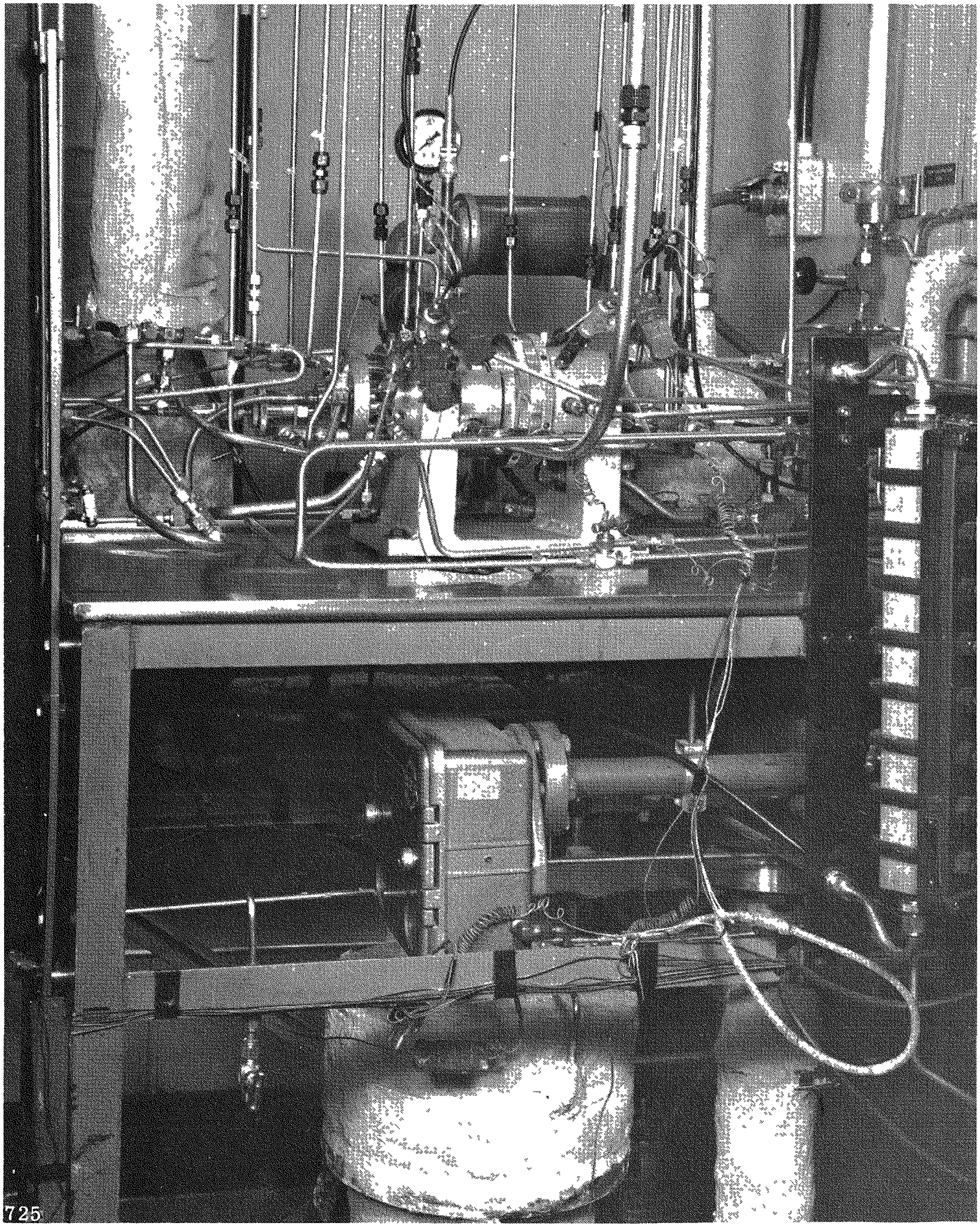


FREE RUNNING BEARING TEST RIG



FIGURE 6-6

## 7.0 CONCLUSIONS

1. Experimental evaluation of the shaft pump, slinger pump, four-vaned impeller pump, and the two blade spiral pump indicated the characteristics, performance, and limitations of each configuration.

2. The four-vaned impeller supplemented by a jet boost stage was selected for the final development to meet the final design requirements.

3. The final mercury pump for the SNAP I system consists of a .4 inch diameter radial flow four-vaned open impeller directly coupled to the turbine shaft and supplemented by a jet boost stage.

4. Analytical and empirical jet-centrifugal pump design procedures were evolved and verified by experimental testing for low specific speed, cavitation -limited, small size, liquid mercury pumps similar to the SNAP I pump.

5. Integration of the jet-centrifugal pump into the turbo-machinery package of the prototype power conversion system was successfully completed.

6. A high level of pump performance was obtained in pump component and pump-bearing subsystem tests, but this level was not completely reproduced in system tests due to non-condensibles, thermal expansions, or contamination of the pump flow passages. System tests with a relatively clean, vacuuum-tight system provided satisfactory pump performance above the design specifications.

7. A pump performance map was generated and the system flow requirements were superimposed on it in order to define a system operating line or point.

## BIBLIOGRAPHY

The reports listed in the bibliography are not available for general distribution. Any inquiries concerning the availability of this information should be directed to the AEC.


| | | |
|---|---|---|
| EN 260 Test Objectives of Pump Rig | 9/30/58 | Secret |
| EN 414 Effects of Increased SNAP I Pump Discharge Pressure | 1/16/59 | Secret |
| EN 452 Operational Characteristics of Jet Centrifugal Pump Hydrosphere Bearing Combination in FRR | 2/11/59 | Secret |
| EN 454 Pump Power and Thrust Evaluation Test Record P-31 | 2/9/59 | Secret |
| EN 600 PTP1 Pump and Bearing Performance | 6/8/59 | Secret |